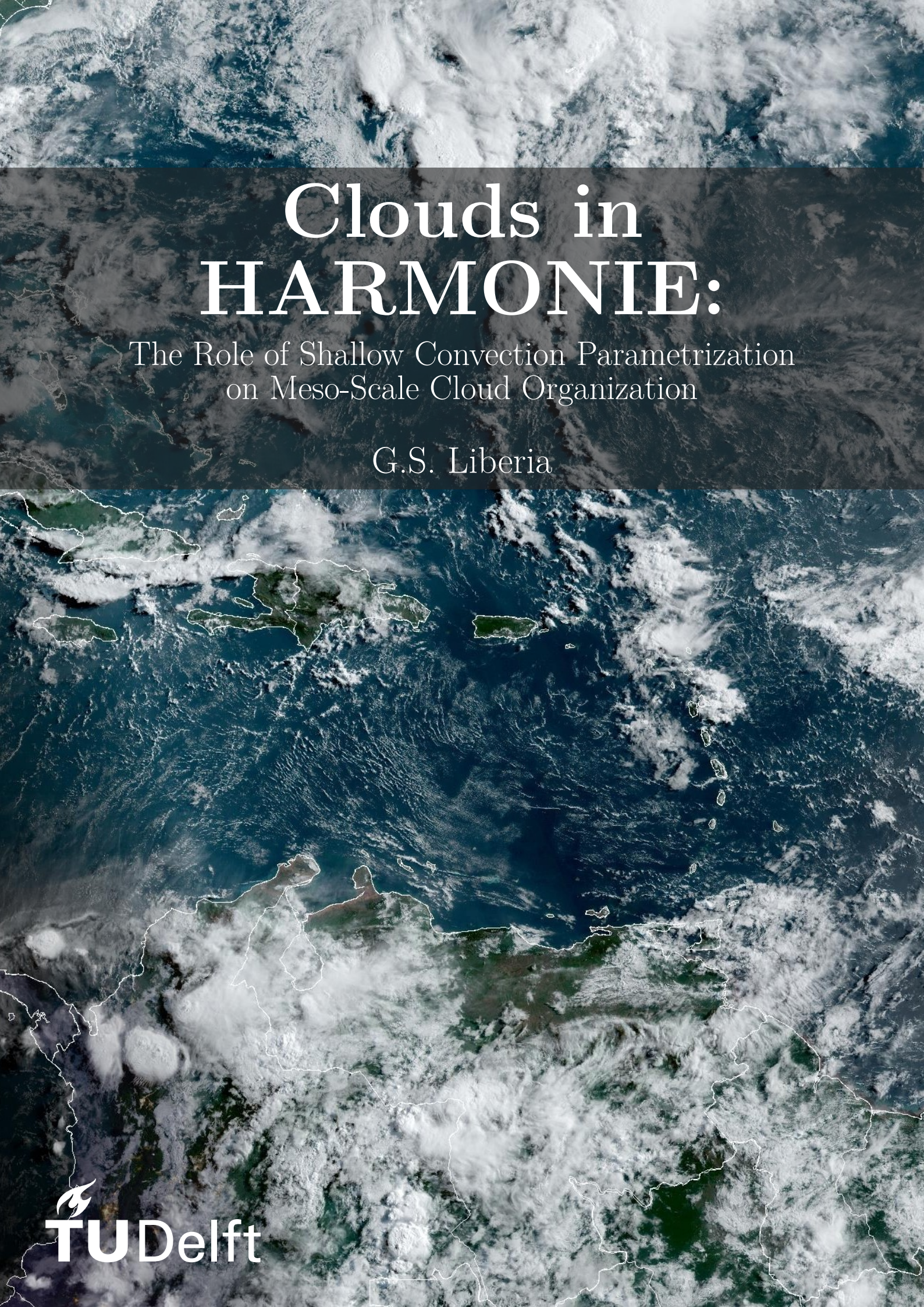

Clouds in HARMONIE:

The Role of Shallow Convection Parametrization on Meso-Scale Cloud Organization

G.S. Liberia

TU Delft

Clouds in HARMONIE:

The Role of Shallow Convection Parametrization on Meso-Scale Cloud Organization

by

Gheylla Liberia

to obtain the degree of Master of Science
at the Delft University of Technology, Faculty of Civil Engineering,
Track: Environmental Engineering,
to be defended publicly on Friday August 25, 2023 at 12:00 PM.

Student number:	4583825	
Project duration:	January 5, 2023 – August 25, 2023	
Thesis committee:	Dr. L. Nuijens,	TU Delft, supervisor
	Prof. Dr. A. P. Siebesma,	TU Delft, supervisor
	Dr. W. de Rooij,	KNMI, thesis committee
	Dr. F. Lopez-Dekker,	TU Delft, thesis committee

Cover: NOAA GOES-East GEOCOLOR COMPOSITE Caribbean

An electronic version of this thesis is available at `http://repository.tudelft.nl/`.

TU Delft

Acknowledgements

I cannot express enough gratitude to my committee for their continued support and encouragement: Dr. A.A. Louise Nuijens, Prof. dr. A. Pier Siebesma and Dr. Wim de Rooij. To Dr. Louise Nuijens, I extend my thanks for your time and your expertise on the subject, as well as for raising numerous questions during our several meetings. To Prof. dr. Pier Siebesma, thank you for your knowledge and great enthusiasm, as well as your involvement in engaging me in diverse conversations related to the subject. To Dr. Wim de Rooij, I'd like to express my gratitude for your ongoing feedback and insights regarding the project and its model. I am extremely grateful to have had the opportunity to have worked alongside exceptional researchers.

I also want to extend my heartfelt gratitude to Alessandro Savazzi, who consistently provided assistance and addressed any questions and concerns I had from the very first meeting. Thank you for your endless support and patience, structure and encouragement.

I'd also like to acknowledge Martin Janssens for his willingness to assist, share his expertise on the subject, and contribute to programming efforts and the individuals at KNMI and ECMWF who have contributed to the development of the model and conducted a range of experiments. Your commitment and time are truly valued.

Lastly I would like to thank my partner; Suenley Paulina. Thank you for always being there and for your unwavering support and encouragement during the times I required it the most. My parents; Suzette Liberia-Veeris and Carlos Liberia, words cannot convey my appreciation for your hard work and dedication. Without you I would not be here today. And to my sister; Suheiley Liberia, thank you for always believing in me.

Gheylla Liberia

Cloud by Tannu Taneja

Clouds
I wish I were a cloud.
I could scream so loud.
Every day I would be of different shape,
once a greedy fox, then a sour grape.
Sprinkling water would be so much fun.
Scolding, yelling, there would be none.
Playing with stars and moon,
hiding the sun at noon.
I wish I were a cloud.
Blue sky all around.

Abstract

Clouds play a crucial role in Earth's systems, influencing the radiation budget and the hydrological cycle. However, their dynamics are poorly represented in climate models, leading to uncertainties in predicting global temperature changes. To better understand cloud dynamics and improve model parametrizations, the large-scale field campaign $EUREC^4A$ focused on studying cloud organization and its potential impact on climate feedback in the North Atlantic trade-wind region, where shallow marine cumulus clouds are prevalent. Within the $EUREC^4A$ framework, this study focuses on cloud fields and organization in the HARMONIE weather model to assess the impact of shallow convective parametrizations on its outputs. By comparing three experiments denominated as 'HARMONIE noHGTQS', HARMONIE noHGTQS noSHAL' and 'HARMONIE noHGTQS noUVmix' one can identify discrepancies and determine what the impact of the various shallow convective parametrizations are. Several cloud organization metrics have been computed for the HARMONIE experiments as well as GOES-16 satellite snapshots. The results show that none of the experiments precisely capture the observed diurnal patterns successfully. There exist disparities in cloud cover, cloud quantity, cloud sizes, and the organization index. Removing shallow convective parametrization partly improves the representation of clouds. It exhibits a stronger correlation with the observed cloud cover data from ceilometer measurements and demonstrates a higher capability to replicate the amount of cloud entities seen in observations in comparison to the other experiments. Furthermore, disabling shallow convection leads to instability and deeper clouds. On the other hand momentum mixing alone has a small impact on clouds, yet it alters wind patterns, resulting in reduced speeds, and little production of precipitation. Overall the model struggles to reproduce detailed cloud patterns such as sugar, mainly due to its coarse resolution. However, it does exhibit a degree of day-to-day variability in cloud patterns. To gain a deeper understanding on the role of parametrized shallow convection, further investigation into model configurations, momentum mixing dynamics, and hybrid approaches are proposed.

Contents

Acknowledgements i

Abstract iii

List of Figures viii

1 Introduction & Motivation 1
- 1.1 Cloud Dynamics . . . 1
- 1.2 EUREC4A . . . 1
- 1.3 HARMONIE . . . 3
- 1.4 Outline . . . 3

2 Research Objectives 4

3 Literature Review 5
- 3.1 Cloud Organization Patterns . . . 5
- 3.2 Pattern Classification Methods . . . 6
- 3.3 Diurnality of Meso-Scale Cloud Organization . . . 7

4 Data & Methods 9
- 4.1 Model Data . . . 9
  - 4.1.1 Experiments . . . 9
  - 4.1.2 Shallow convection . . . 10
  - 4.1.3 UV wind mixing . . . 11
- 4.2 Observational Data . . . 12
- 4.3 Research Methods . . . 12
  - 4.3.1 Cloud Metrics . . . 12
  - 4.3.2 Cloud Mask . . . 14
  - 4.3.3 Day-to-day variability . . . 15

5 Results & Discussion 16
- 5.1 Cloud Behaviour . . . 16
  - 5.1.1 Low cloud cover . . . 16
  - 5.1.2 Size of voids . . . 19
  - 5.1.3 Number of cloud entities . . . 21
  - 5.1.4 Size of cloud entities . . . 22
  - 5.1.5 Organization index . . . 23
- 5.2 What is the cause for the various disparities? . . . 26
  - 5.2.1 Water Balance . . . 26
  - 5.2.2 CAPE . . . 26
  - 5.2.3 Up- and downdraft strengths . . . 28
  - 5.2.4 Precipitation . . . 30
  - 5.2.5 Humidity . . . 31
  - 5.2.6 Buoyancy & Winds . . . 32
- 5.3 Visual organization . . . 35

6 Conclusions & Recommendations 37

A Metrics Complete Time-Series 40

List of Figures

1 Overview of the EUREC4A Research Domain. Retrieved From the EUREC4A Website. . . . 2
2 Overview of Cloud Categorizations. Retrieved and edited from *Clouds, circulation and climate sensitivity* [3]. . . . 2
3 Sugar, Gravel, Fish and Flowers meso-scale cloud patterns in the trade-winds. Images retrieved from "Sugar, gravel, fish and flowers: Mesoscale cloud patterns in the trade winds" [18]. . . . 6
4 Example of Mixing of The Atmosphere. Warm Air Moves Up and Cold Air Comes Down (Right Panel), Slow Winds Move Up and Fast Winds Come Down (Right Panel). Figures Retrieved From: *Transport in the Atmosphere-Vegetation-Soil Continuum* [38]. . . . 11
5 Vertical Profile of Wind Speed (Left Panel) and Potential Temperature (Right Panel) of a Well Mixed Atmospheric Boundary Layer (ABL). Figures Retrieved From *Transport in the Atmosphere-Vegetation-Soil Continuum* [38]. . . . 11
6 Vertical Profile of Total Wind Speed of a Stratified Atmosphere. Figures Retrieved From *Transport in the Atmosphere-Vegetation-Soil Continuum* [38] . . . 12
7 Categorization of The Various Types of Cloud Distribution Within a Cloud Field. Clustered (Left Panel), Regular (Middle Panel), Random (Right Panel). . . . 13
8 Iorg Cumulative Density Function Graph with Cloud Organization Categorizations. Retrieved From "Organization of tropical convection in low vertical wind shears: Role of updraft entrainment" [44]. . . . 13
9 Density Plot of Individual Pixel Cloudiness . . . 14
10 Cloud Mask Example: Transition From Original HARMONIE Low Cloud Cover Outputs (Left Panel) to Binary Cloud Mask (Right Panel). . . . 14
11 Composite Diurnal Cycle of Low Cloud Cover Computed With the Cloud Organization Metric Algorithm. . . . 16
12 Composite Diurnal Cycle of Cloud Fraction From the HARMONIE Model Output for the Control Experiment. . . . 17
13 Composite Diurnal Cycle of Cloud Fraction From the HARMONIE Model Output for the No_conv Experiment. . . . 18
14 Composite Diurnal Cycle of Cloud Fraction From the HARMONIE Model Output for the No_mom Experiment. . . . 18
15 Density Plot of Cloud Top . . . 19
16 Composite Diurnal Cycle of Open Sky Computed With the Cloud Organization Metric Algorithm. . . . 19
17 Correlation of Cloud Cover and Open Sky for the 'Control' (a), the 'No_conv' (b), 'No_mom' (c) and GOES-16 Observations (d). . . . 20
18 Composite Diurnal Cycle of Number of Objects Computed With the Cloud Organization Metric Algorithm. . . . 21
19 HARMONIE Snapshot of Low Cloud Cover at Time 2020-02-02T06:00:00 for 'Control' (Left Panel), 'No_conv' (Middle Panel), 'No_mom' (Right Panel). . . . 21
20 Composite diurnal cycle of mean length scale, mean perimeter length and maximum length scale. . . . 23
21 Composite Diurnal Cycle of Cloud Organization Index (Iorg) Computed With the Cloud Organization Metric Algorithm. . . . 24
22 Composite Diurnal Cycle of Cloud Organization Index (Iorg) Computed from LES simulations produced by Alessandro Savazzi. . . . 24
23 Density Plot of Convective Available Potential Energy (CAPE) for all of the HARMONIE experiments. . . . 27

24 Composite Diurnal Cycle of Convective Available Potential Energy (CAPE) for all of the HARMONIE experiments. . . . 27
25 Mean Vertical Profile of Up- and Downdrafts (W-Wind speed) for all of the HARMONIE Experiments. . . . 29
26 Mean Vertical Profile of Cloud Fraction (CF) (Left Panel), Total Liquid Water (Middle Panel), In-Cloud Water (Right Panel) for all of the HARMONIE Experiments. . . . 29
27 Composite Diurnal Cycle of Precipitation . . . 30
28 Mean vertical profile of specific humidity. . . . 31
29 Mean Vertical Profile of Liquid Water Potential Temperature Flux (Θ_l flux). . . . 32
30 Composite Diurnal Cycle of Total Surface Wind speed for all of the HARMONIE Experiments. . . . 33
31 Mean Vertical Profile of East-Ward (U) Winds (Left Panel) and North-Ward (V) Winds (Right Panel). . . . 34
32 HARMONIE Snapshot of Low Cloud Cover for Control (Left Panel), No_conv (Middle Panel), No_mom (Right Panel) at Time 2020-02-02T12:00:00. . . . 35
33 HARMONIE Snapshot of Low Cloud Cover for Control (Left Panel), No_conv (Middle Panel), No_mom (Right Panel) at Time 2020-02-02T20:00:00. . . . 35
34 HARMONIE Snapshot of Low Cloud Cover for Control (Left Panel), No_conv (Middle Panel), No_mom (Right Panel) at Time 2020-02-03T02:00:00. . . . 36
35 Complete Time-Series of the Low Cloud Cover Metric Using the Cloud Organization Algorithm. . . . 40
36 Complete Time-Series of the Open Sky Metric Using the Cloud Organization Algorithm. . . . 41
37 Complete Time-Series of the Number of Objects Metric Using the Cloud Organization Algorithm. . . . 42
38 Complete Time-Series of the Mean Length Scale Metric Using the Cloud Organization Algorithm. . . . 42
39 Complete Time-Series of the Mean Perimeter Length Metric Using the Cloud Organization Algorithm. . . . 43
40 Complete Time-Series of the Maximum Length Scale Metric Using the Cloud Organization Algorithm. . . . 43
41 Complete Time-Series of the Cloud Organization Index Metric Using the Cloud Organization Algorithm. . . . 44

1 Introduction & Motivation

1.1 Cloud Dynamics

Clouds have a dominant role in several processes of the Earth's systems. They not only affect the Earth's radiation budget, regulating the average surface temperature but also play an important role in the hydrological cycle through the generation of precipitation [1, 2]. Despite this, the understanding of cloud dynamics is still limited and are therefore poorly represented within climate models [3–5]. While most general circulation models are able to capture the magnitude of global warming, they are unable to agree on the induced changes in cloud properties, mainly due to shallow marine cumulus clouds [3, 5], hereby producing a diverging prediction of the global mean equilibrium surface temperature in response to the doubling of CO_2 of 1.5K to 4.5K [6].

Several important atmospheric processes are too small to be captured by current model resolutions, thus they require parametrization schemes [7, 8]. Parametrizations use simplified equations that are functions of resolved prognostic variables and are designed to represent the mean effect of the sub-grid processes [8]. Because these parametrizations are simplifications of often poorly understood processes, most uncertainty in the global circulation models can be attributed to them [9]. Climate models will always have to operate with the use of parametrizations [8]. However, the uncertainties produced by these parametrizations can be reduced by having a better scientific understanding of the physical processes that are happening and incorporating these within the model parametrization schemes.

1.2 EUREC4A

One of the many ways to better understand the dynamics of clouds and potentially produce more accurate parametrizations is to understand the underlying cause of their organization. This entails understanding the distribution of clouds in an area rather than the formation of individual clouds.

Study of clouds started a long time ago in 1802 when Luke Howard decided to categorize single clouds based on their outward characteristics. Later on, these categorizations were expanded to inform about their altitude and the way they formed. These categorizations are still widely used in studies of meteorology and can be found in the *International Cloud Atlas* [10]. Studies on stratocumulus clouds revealed that clouds can organize in peculiar ways such as, but not limited to, cloud streets, open and closed cells, fronts and cyclones [4]. In recent years also the organization of shallow marine cumulus clouds received attention, for their influence on low cloud climate feedback.

Various field campaigns measured the North Atlantic trade-wind cumuli with the aim of gaining a deeper comprehension of the cloud dynamics and structure of the atmosphere in this region [11–13]. These efforts resulted in a collection of data which was not readily available before, enhancing our understanding of the ongoing processes such as cloud transition and precipitation. The most recent and extensive field campaigns carried out in this area is called ; 'Elucidating the Role of Clouds-Circulation Coupling in Climate', EUREC4A [14]. Its primary objective was to expand our knowledge regarding the intricate interactions of the interplay between clouds, convection and circulation and their role in climate change [15].

The observations took place just eastward of Barbados because the clouds observed in this particular area were considered representative of the clouds found across the broader trade-wind region [16]. The entire domain is visually presented as the solid red rectangle in Figure 1. Shallow convective clouds are the most prevalent in the subtropical and anticyclonic regions

[17]. These clouds are generally 1500-2000m thick at peak development and are based at about 600-760m altitude, see Fig. 2.

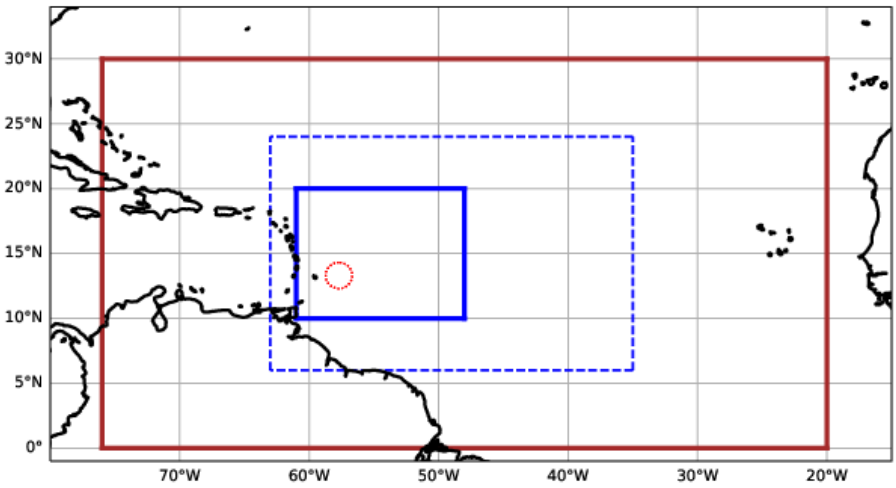

Figure 1: Overview of the EUREC4A Research Domain. Retrieved From the EUREC4A Website.

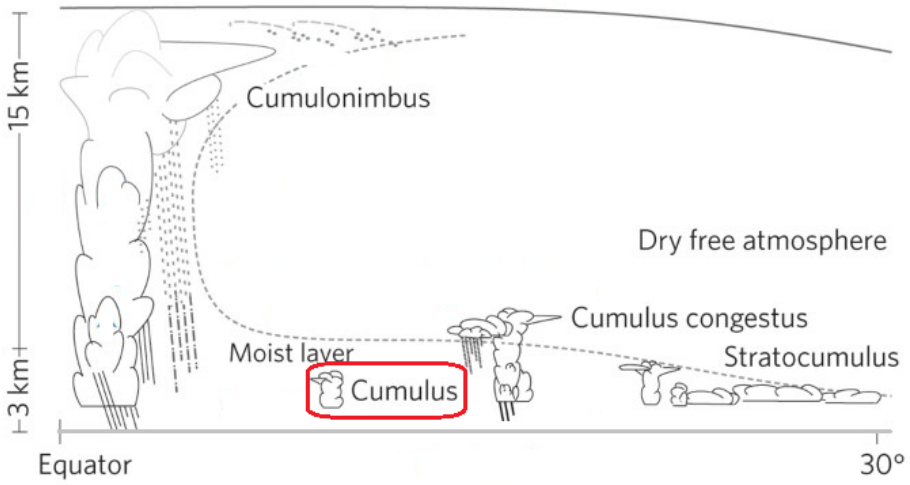

Figure 2: Overview of Cloud Categorizations. Retrieved and edited from *Clouds, circulation and climate sensitivity* [3].

The research period was from 1 January 2020 to 1 of March 2020, during the boreal winter, when the intertropical convergence zone is the most southern [18]. This period is characterized by prevailing trade-winds and moderate large-scale subsidence, also considered as the typical trade-wind conditions where shallow convection is present [19, 20]. Overall, this research effort has provided significant data for the understanding of cloud dynamics and serves as a stepping stone for further exploration into the intricate relationship between clouds, circulation patterns, and climate change.

1.3 HARMONIE

Numerical models are the foundation of climate change studies. To accurately model the current climate and weather as well as future climate predictions, it is essential to understand the physical mechanisms governing cloud dynamics in the real world [3]. There have been several efforts made to assess the accuracy of numerical models in replicating observed cloud dynamics, organization, and precipitation, in an attempt to find the causes of the model errors and improve climate predictions. The data collected during $EUREC^4A$ has played a crucial role in advancing this research.

A previous research endeavor from Voort [21], which this report aims to expand on, was centered on assessing how well the HIRLAM ALADIN Research on Meso-scale Operational Numerical Weather Model (NWP) in Europe, known as HARMONIE, represents subtropical marine clouds [21]. This NWP is currently in use by the 'Koninklijk Nederlands Meteorologisch Instituut' (KNMI) for weather forecasting across Europe. In addition, since 2018, HARMONIE has been implemented in the trade-wind region to explore its capacity to effectively simulate cloud formations. This initiative aims to assess its suitability for future climate predictions.

Voort centered their investigation on several experiments from HARMONIE cycle 40, specifically focusing on cloud and atmospheric profiles up to 3 km. They compared the results of these experiments to observational data gathered during $EUREC^4A$. Their objective was to assess the accuracy of HARMONIE in replicating the atmospheric structure within the trade-wind region. However, the study did not extensively analyze cloud patterns. In this subsequent research, we aim to delve deeper into the intricacies of cloud patterns.

1.4 Outline

In this work, chapter 2 discusses the research objective. Following this, Chapter 3 conducts a literature review, exploring research on cloud patterns and discussing numerical weather prediction models. Once the research's groundwork is established, Chapter 4 elaborates on the domain, data sources, and methodology employed. The study's findings are then presented in Chapter 5. Lastly, Chapter 6 presents the summary and conclusions, where the research outcomes are interpreted in the context of existing knowledge and recommendations are given for future research.

2 Research Objectives

The primary aim of this research is to assess how shallow convective parametrizations used in HARMONIE affects cloud fields and cloud organization properties.

By comparing different experiments and identifying any discrepancies that arise, the study seeks to gain valuable insights into the performance and limitations of the model's cloud representation. Understanding the reasons behind the observed deviations will be crucial for refining and improving the convective parametrization schemes, ultimately enhancing the accuracy of HARMONIE's cloud simulations. In order to efficiently conduct this research the following 3 questions are answered:

1. **How well can HARMONIE reproduce the observed meso-scale cloud organization?**

2. **How does the shallow convection parametrization scheme influence the cloud climatology? And what are the reasons for these differences?**

3. **Is HARMONIE visually able to simulate the Sugar, Gravel, Fish and Flower cloud structures? And is HARMONIE able to simulate their day-to-day variation?**

3 Literature Review

3.1 Cloud Organization Patterns

Cloud organization can have a major influence on the Earth's climate, as it can impact the amount of radiation reflected or absorbed by the planet's surface. Additionally, the manner in which clouds are arranged can affect the water cycle by regulating the quantity of water vapor transported from the Earth's surface to the atmosphere. Research suggests that the clustering of clouds has a different feedback on the climate compared to randomly organized cloud fields [22]. These distinctions in feedback reinforce the significance of understanding cloud patterns and the reasoning behind their organization.

There can be various causes for cloud organization and patterning. From satellite images one can observe cloud fields can have various spatial patterns that are made up from individual clouds that are similar or from regular sequences of changing clouds [18]. However, in some cloud fields, patterns are not as clear, specifically in the region of the North Atlantic where shallow cumulus are the prominent cloud type. In this region of the world there is still lots to discover when it comes to the diversity of cumulus fields considering the wide range of conditions they can be found in [23].

Due to the incomplete comprehension of cloud dynamics in this particular area and recognizing the significance of these clouds in the climate feedback loop, several field campaigns ([15, 24]) have been conducted in order retrieve information of the atmospheric structure with the aim to advance the understanding of the interplay between clouds, convection and circulation and their role within climate change [15]. Previous studies have highlighted the significance of deep convection organization in regulating the Earth's heat-loss to space. However, our understanding of shallow convection remains limited, prompting a growing interest in investigating this phenomenon and seeing if similar processes are visible. In particular, researchers are focusing on understanding the types of cloud patterning that exist in the trade-wind region.

One paper that has gained much attention is Stevens et al. paper on Sugar, Gravel, Fish and Flower meso-scale patterns. It has been focused on determining whether a spatial patterning of meso-scale cloud organization can be detected through visual inspection in the North Atlantic Trades, and if so how often these patterns reappeared [18]. Here from it was concluded that four main patterns could be observed. These were named; Sugar, Flower, Fish and Gravel and are described as follows [18]:

- **Sugar**: Very fine scale clouds, similar to the dusting of powdered sugar, hereby the name Sugar. They have a small vertical extent and little evidence of self organisation.
- **Gravel**: Fields containing clouds along a line or arcs with sizes in the order of meso-β (20km to 100km).
- **Fish**: Cloud fields resembling the fish-bone structure. They are meso-α networks that are separated from each other or other cloud forms.
- **Flower**: Irregularly shaped meso-β scale (20km to 200km) stratiform clouds, appearing in bunches. They are well separated from each other by regions of devoid clouds.

A visual depiction of these patterns is presented in figures 3. For a detailed explanation of the classification methods and conclusions see "Sugar, gravel, fish and flowers: Mesoscale cloud patterns in the trade winds".

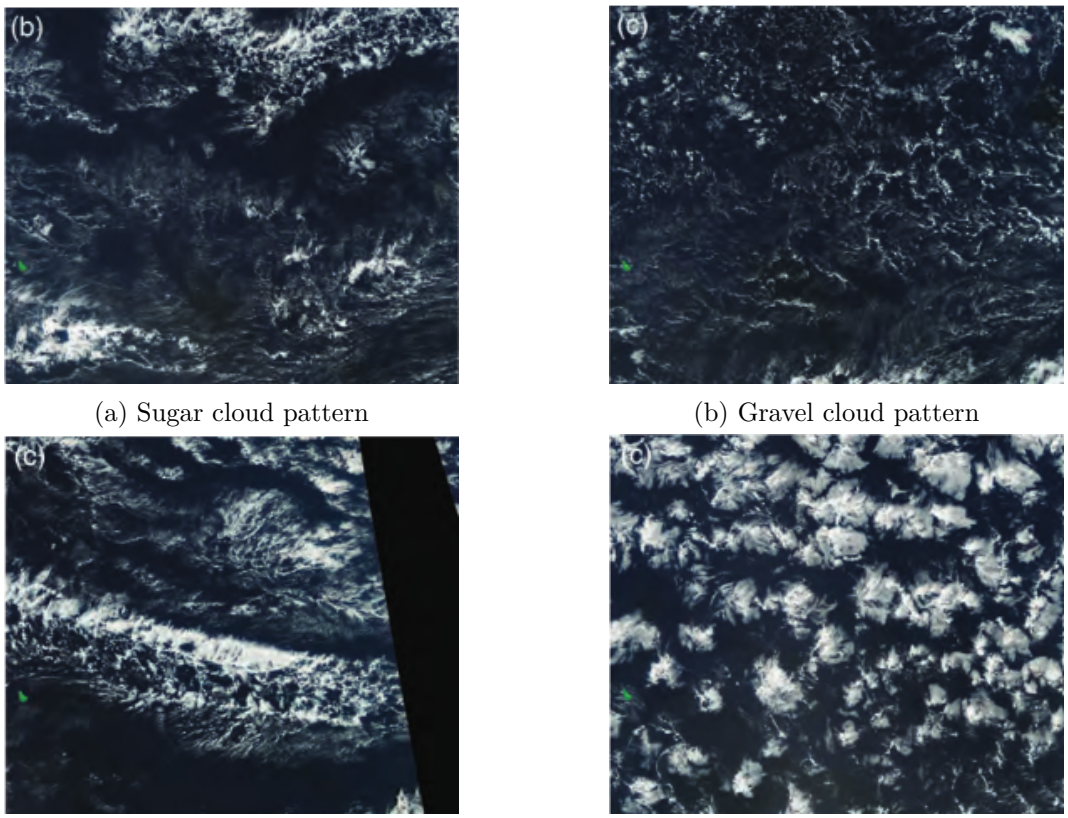

(a) Sugar cloud pattern

(b) Gravel cloud pattern

(c) Fish cloud pattern

(d) Flowers cloud pattern

Figure 3: Sugar, Gravel, Fish and Flowers meso-scale cloud patterns in the trade-winds. Images retrieved from "Sugar, gravel, fish and flowers: Mesoscale cloud patterns in the trade winds" [18].

3.2 Pattern Classification Methods

The discovery of these four meso-scale cloud organization patterns in the North Atlantic trade-wind region has been the only one of its kind. While it is has been revolutionary for the world of atmospheric sciences, the classification methods used were rather subjective. Consequently, others have been inspired to develop more objective methods to not only identify the four patterns that were discovered in Stevens et al., but also try to identify general convection patterns present within the trade-wind region.

Denby has been the first to try and detect general patterns in satellite images through the use of trained unsupervised neural networks [25]. The concept is to construct a computational model that is capable of automatically and without supervision group images that contain similar cloud structures. In this manner the model is not taught which pattern it needs to detect but it can rather objectively detect similarities based on metrics such as cloud cover and size. The results show that the neural network has been successful in identifying and grouping images containing similar cloud structures without supervision. This allows for objective study of very large data-sets [25].

As opposed to Denby, Rasp et al.'s work has been focused on trained neural networks for the categorization of organization of shallow cumulus convection in the trade-wind region [26]. The four patterns that were detected by Stevens et al. are used to train deep learning algorithms making it possible to automate the detection of patterns. Herein the algorithm is not able to work autonomously, but is rather trained to detect a correct pattern.

Lastly, from these methods the most interpretable yet still objective way to detect organizational patterns is based on the principal choice analysis as conducted by Janssens et al. Herein, 21 different cloud organization metrics, divided into the following three methodological categories: statistical moments of physical cloud properties, object based metrics and attributes of scale decompositions, are diagnosed. By using the principal component analysis the complete set of metrics is reduced to a smaller subset of metrics that are able to produce the maximum variance [27]. They found that the cloud patterns can be effectively described as a four-dimensional combination of characteristic length, void size, directional alignment, and cloud top height variance. The description is objective and interpretable, allowing for a better understanding of cloud organization compared to other methods like unsupervised machine learning or human pattern identification [27].

While all of the research mentioned above use different methods for meso-scale cloud organization detection, they all have the same objective, to objectively be able to detect patterns within shallow cumulus cloud fields in order to be able to better understand the dynamics of cloud processes and ultimately determine how clouds will react to a warming climate.

3.3 Diurnality of Meso-Scale Cloud Organization

The daily cycle stands as one of the most fundamental modes of tropical climate variability [28] , exerting a profound influence on various meteorological and climatic processes. In the context of meso-scale cloud organization, gaining insights into the factors responsible for their daily variations is of major importance. As climate change continues to exert its influence, understanding the daily variability in meso-scale cloud organization becomes increasingly crucial for accurately predicting weather phenomena, monitoring climate trends, and mitigating the impacts of changing climatic conditions on tropical ecosystems. Based on the results produced by Stevens et al. several researchers have been focused on understanding the daily variability in meso-scale cloud organization within the trades.

The studies conducted by Vial et al. have provided valuable insights into the daily variability of cloudiness and shallow cumulus activity within the trade-wind region [29] [28]. The findings show that the level of cloudiness and cumulus activity tends to reach its peak in the late evening, gradually decreasing to its lowest point during the afternoon [28, 29]. This diurnal cycle is characterized by the presence of two distinct cloud populations. The first population emerges during the daytime and comprises non-precipitating small and shallow cumulus clouds scattered in a regular pattern. In contrast, the second population appears during the nighttime, exhibiting fewer but deeper clouds that have a higher likelihood of precipitation. The regular pattern of small and shallow cumuli during the day and the organized arcs of deeper precipitating clouds at night offer intriguing insights into the dynamic nature of cloud behavior in response to changing solar radiation and atmospheric conditions.

These diurnal patterns in cloud cover can be related to the type of cloud pattern, which in turn relates to the size of cloud objects. It can be observed that specific cloud patterns exhibit distinct preferences for certain times of the day. The patterns fish and sugar which are smaller fine cloud structures, are mostly observed during the day. These smaller cloud objects scatter in a regular pattern across the atmosphere, contributing to the overall cloud cover during daylight hours. On the other hand, as night falls, the gravel and flowers patterns become more prominent. These patterns consist of deeper and larger cloud clusters that organize themselves into extensive arcs and organized systems during the night, leading to a peak in cloud cover during this time [28].

This daily variation cannot be attributed to the sea surface temperature (SST) as this does not present variations during the daily cycle due to the strong wind mixing present within the trade-

wind region [29]. Instead, these variations in cloud cover are likely driven by variations in the intensity of shallow convection, highlighting the significant influence of cloud convection coupling in this region [30]. The diurnal cycle can be interpreted as a result of either an increase in surface winds and buoyancy fluxes during the night or an enhancement in radiatively driven instability across the entire cloud layer. Both of these processes can reinforce turbulent and convective transports of heat and moisture within the boundary layer, contributing to the dynamic nature of cloud behavior throughout the day [29].

4 Data & Methods

To conduct the research, multiple sets of data are necessary. These include the model data, which consists of information generated by the weather model being used, and the observational data, which encompasses real-world measurements. The process of acquiring and handling these data sets is explained in detail within this section.

4.1 Model Data

Several characteristics of the atmosphere such as, air movement, temperature and moisture, can be interpreted by using hydrodynamic equations. These are a set of non-linear equations that do not have analytical solutions resulting in the use of numerical integration in order to find approximations of the true solution. This involves breaking the atmosphere into grids of smaller cells and applying these equations to each cell, developing a numerical weather model. These numerical models have the ability to forecast future weather by using information about the current state of the atmosphere by extrapolating the computed tendencies of these variables into the future. Besides the original differential equations, numerical weather models make use of discretized equations that describe sub-grid processes with certain spatial and temporal scales resulting in the need for parametrizations, where only their statistical effects on the mean flow are taken into account [31].

As previously discussed in the introduction, this research centers on the HARMONIE cycle 43 numerical weather model currently in operation by the KNMI. It is a regional high-resolution meso-scale convection permitting model with a non-hydrostatic dynamical core and is currently mainly used for short-range weather forecasts from 0 up to 2 days. It has a horizontal resolution of 2.5 km, which enables it to accurately simulate processes that are crucial for cloud formation and precipitation. Moreover, it has 65 vertical levels and is able to produce hourly outputs up to 48-hour forecast lengths [31].

All model data used for this research are outputs from the experiments of HARMONIE. The data covers the time frame from January 1 2020, to March 1 2020. The experimental outputs were obtained from the KNMI. The research is focused on the North Atlantic trade-wind region. Within HARMONIE this is a specific sub-field of the broader domain. The geographical region under investigation precisely matches one of the sub-regions explored during $EUREC^4A$ [32] specifically; 10°N - 20°N, 48°W - 58°W and is visualised as the solid blue rectangle in Figure 1.

4.1.1 Experiments

The model experiments utilized to carry out this research are climate runs. This involves initializing the model with specific conditions and then allowing it to run freely without reinitialization for a continuous duration of one month. Various configurations can be used to run HARMONIE. By deactivating or modifying settings such as shallow convection, surface conditions and wind mixing it is possible to asses the impact of the variables of interest.

HARMONIE cycle 43 is an updated version of the prior developed and currently in use HARMONIE cycle 40, which was updated mainly to improve the cloud scheme that had a tendency to underestimate low cloud cover [33]. To resolve this problem, an additional variance term was added to incorporate more variability within the humidity scheme. However, studies revealed that the addition of this additional variance term caused HARMONIE cycle 43 to produce unrealistic values of cloud cover, overestimating it by a factor of approximately 1.8 [34]. Motivated by these results, it was decided not to implement the additional variance term and instead concentrate on experiments that do not include this, such as:

Table 1: HARMONIE experiments overview. SCP = Shallow Convective Parametrization, UVP = UV Mixing (Within Shallow Convective Parametrization).

	Experiment Name	**Alternate Label**	**Specifications**
1	HARMONIE noHGTQS	Control	ECUME 6 Height QS = FALSE SCP = TRUE UVP = TRUE
2	HARMONIE noHGTQS noSHAL	No_conv	ECUME 6 Height QS = FALSE SCP = FALSE UVP = FALSE
3	HARMONIE noHGTQS noUVmix	No_mom	ECUME 6 Height QS = FALSE SCP = TRUE UVP = FALSE

4.1.2 Shallow convection

When parcels of air are warmer than the surrounding environment they are less dense and will have the tendency to rise due to increased buoyancy. This process is denominated as convection. Once these air parcels reach a certain altitude where the temperature and pressure conditions are suitable for their water vapor content to condense, convective clouds are formed[35]. Generally, when vertical motions are powerful enough to be able to transport air parcels from the lower atmosphere to 500hPa, due to thermally driven turbulent mixing, this is considered deep convection. In contrast, when the parcels are unable to reach 500hPa, it is classified as shallow convection [36].

At 2.5 km resolution HARMONIE is expected to run with resolved deep convection explicitly represented by the model's non-hydrostatic dynamics; eliminating the need for parametrization of deep convection. However, since shallow convection occurs at a smaller scale, parametrization hereof is still required. This is done by using an eddy-diffusivity mass-flux (EDMF) framework consisting of one or more updrafts, transporting heat, moisture and momentum [37]. The level at which the clouds attain neutral buoyancy with respect to their surroundings marks their cloud top, which in the case of shallow convection in HARMONIE is below 3000m above the surface [17].

Shallow convective mixing aims to create a uniform composition of the atmospheric boundary layer. Warm air, slow winds, and moist air near the surface are uplifted, while simultaneously, colder air, stronger winds, and drier air aloft are brought downwards. This process is shown in Figure 4.

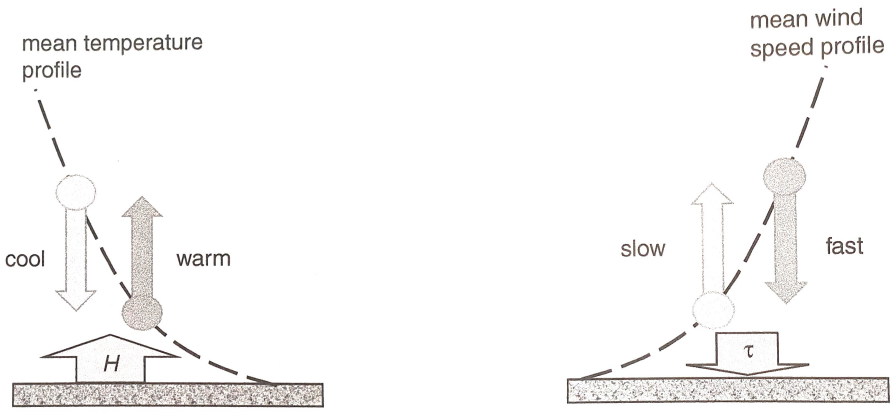

(a) (b)

Figure 4: Example of Mixing of The Atmosphere. Warm Air Moves Up and Cold Air Comes Down (Right Panel), Slow Winds Move Up and Fast Winds Come Down (Right Panel). Figures Retrieved From: *Transport in the Atmosphere-Vegetation-Soil Continuum* [38].

This mixing through shallow convection creates turbulent eddies within the atmosphere, effectively stirring and homogenizing the entire atmospheric boundary layer. This process leads to a stable thermodynamic state with a well-mixed vertical structure [39]. Figure 5 visually illustrates the general vertical profile of such a well-mixed atmospheric boundary layer.

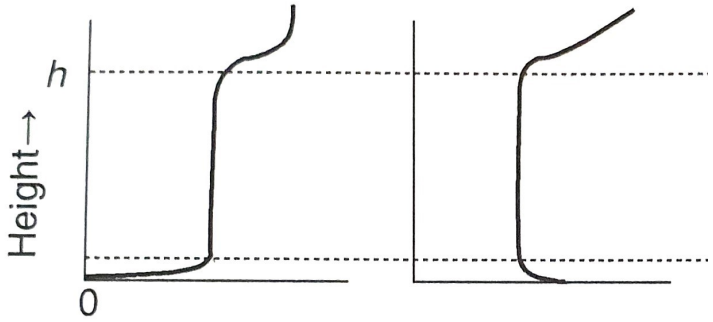

Figure 5: Vertical Profile of Wind Speed (Left Panel) and Potential Temperature (Right Panel) of a Well Mixed Atmospheric Boundary Layer (ABL). Figures Retrieved From *Transport in the Atmosphere-Vegetation-Soil Continuum* [38].

Limited research has been conducted on the effect of turning off shallow convective parametrization within convection permitting weather models. According to Khain et al., if shallow convection is disabled within a convection permitting numerical weather model, the updrafts would intensify causing more occurrences of high CAPE. Furthermore, due to a lack of vertical mixing the environment would become more unstable. This can result in the formation of localized and scattered convection patterns over the domain, as well as the potential for the development of intense and deep convective systems and more precipitation [40].

4.1.3 UV wind mixing

As opposed to the shallow convective parametrization scheme which when disabled, eliminates all transport of temperature, humidity and wind simultaneously, one can disable only the momentum mixing through wind by disabling the UV wind mix. Within HARMONIE the U and V wind components represent the horizontal wind velocities in the eastward (U) and northward

(V) directions, respectively. UV wind mixing is the mixing of these horizontal wind components, through shallow convection. The mixing of U and V winds through shallow convection is achieved by considering the vertical transport of momentum within the shallow layer. As the convective processes occur, parcels of air are uplifted or descend within the boundary layer, affecting the horizontal wind distribution.

As described already instead of turning of all transport modes, only the wind will not be mixed. Consequently turning off the momentum mixing alone will have a much higher impact on the wind. In the absence of an upward motion of slow winds and a downward motion of stronger winds, the vertical profile of wind is expected to exhibit less mixing and more stratification. Instead of a resembling a wind speed profile as presented in Figure 4b, it will bear a closer resemblance to Figure 6.

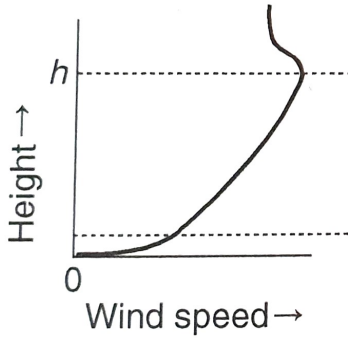

Figure 6: Vertical Profile of Total Wind Speed of a Stratified Atmosphere. Figures Retrieved From *Transport in the Atmosphere-Vegetation-Soil Continuum* [38] .

4.2 Observational Data

In this research, a comprehensive approach is adopted by utilizing both in-situ measurements and satellite data to gather valuable insights. The in-situ data is collected from instruments stationed at the Barbados Cloud Observatory [20]. These in-situ measurements provide direct and localized information about the atmospheric conditions.

For the satellite data, 10 minutes infrared (13 μm) satellite snapshots for the period of 1 January 2020 - 1 March 2020 are taken from GOES-16 satellite. These are retrieved from the channel 13 ABI level 1b: clean infra-red, cloud and moisture data, available on the "NOAA Comprehensive Large Array Data Stewardship System" website [41]. The additional observational data needed for the research is sourced from the intake catalog of the $EUREC^4A$ project.

4.3 Research Methods

4.3.1 Cloud Metrics

To quantitatively assess the level of cloud organization and patterning, the study will calculate specific cloud organization metrics for both the HARMONIE experimental outputs and observational cloud field snapshots. This is done for the entire research period. By analyzing time-series data and composite diurnal cycles, comparisons between the model simulations and observations can be made. For this, the metrics algorithm produced by Janssens et al. will be applied on both HARMONIE as well as the satellite observations [27].

For this research only the following 7 metrics will be discussed and compared:

1. Cloud Cover

2. Open sky (size of voids)
3. Number of objects
4. Mean perimeter length
5. Mean length scale
6. Max length scale
7. Iorg

Most of the metrics presented above target cloud behaviour and size. Given the emphasis on cloud organization, a metric that specifically targets this aspect is Iorg. This is a simple index which aims to classify a cloud field as regular, clustered or random depending on the cloud distribution within the field, see Figure 7 [27, 42, 43].

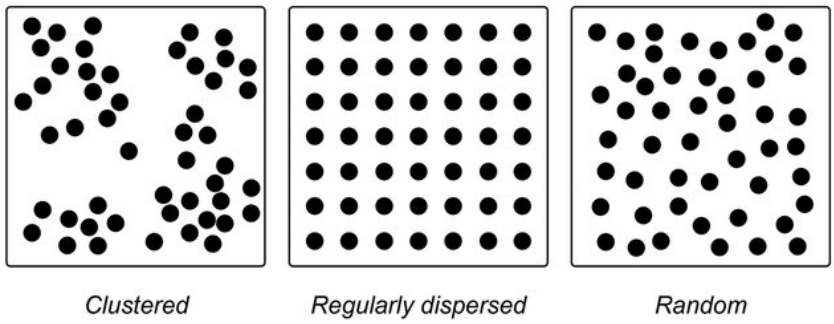

Figure 7: Categorization of The Various Types of Cloud Distribution Within a Cloud Field. Clustered (Left Panel), Regular (Middle Panel), Random (Right Panel).

The geometrical distance from each cloud entity core to the centroid of its nearest neighbor is calculated and a cumulative density function (CDF) of these distances is made. The CDF of the distances are compared to the theoretical random distribution and the area underneath the curve determines the value of Iorg [44]. When Iorg < 0.5 clouds are regularly distributed, Iorg $= 0.5$ denotes a random distribution and Iorg > 0.5 are clusters of clouds, see Figure 8 [44].

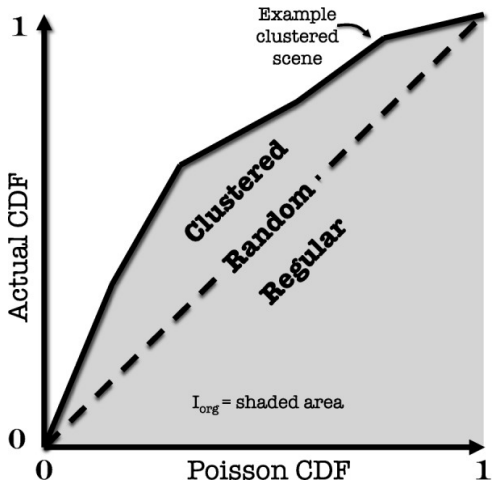

Figure 8: Iorg Cumulative Density Function Graph with Cloud Organization Categorizations. Retrieved From "Organization of tropical convection in low vertical wind shears: Role of updraft entrainment" [44].

4.3.2 Cloud Mask

The algorithm used for the calculation of the various cloud metrics can only operate on a binary (0/1) representation of the cloud field. Consequently a cloud mask has to be computed based on the original cloud field inputs. Because the focus of this research is on low clouds, the low cloud cover output fields from the HARMONIE experiments will be utilized for the creation of their cloud masks. The individual pixel cloudiness of the experiments show a bimodal distribution, see Fig. 9.

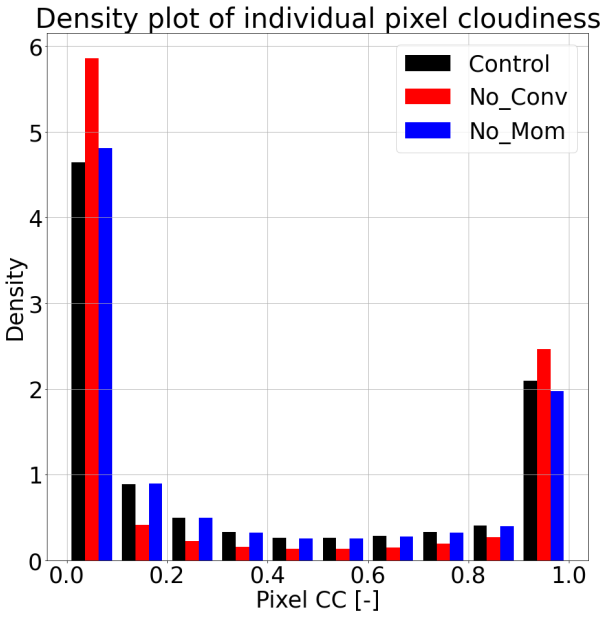

Figure 9: Density Plot of Individual Pixel Cloudiness

From this analysis it was determined that pixels with cloud cover exceeding 0.5 were designated as clouds and marked with a value of 1. Conversely, pixels with cloud cover below 0.5 were considered clear sky areas and were masked with a value of 0. An example of this cloud mask is presented in Figure 10.

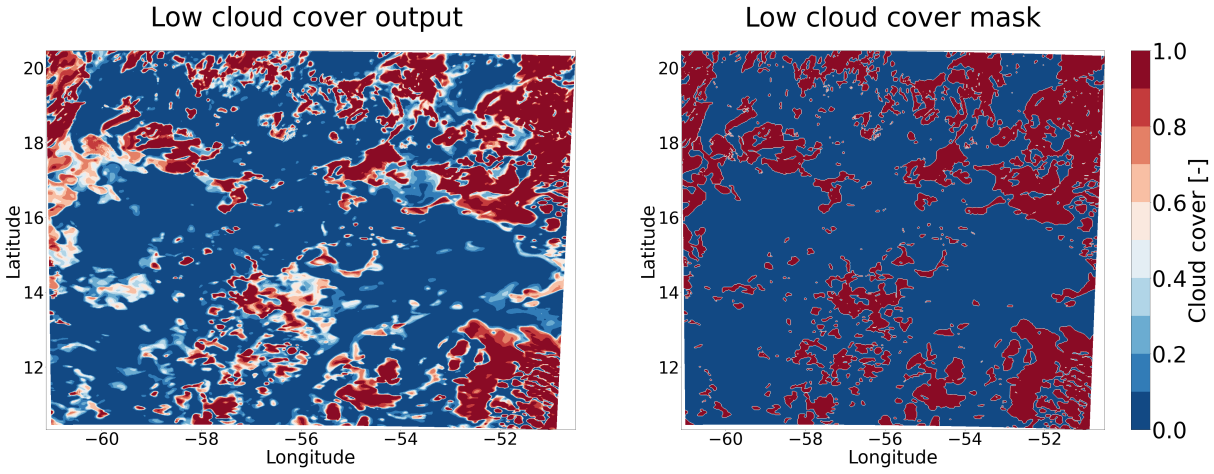

Figure 10: Cloud Mask Example: Transition From Original HARMONIE Low Cloud Cover Outputs (Left Panel) to Binary Cloud Mask (Right Panel).

The GOES-16 cloud and moisture data are classified based on their brightness temperatures. Brightness temperatures between 277 and 290K are regarded as clouds. The lower threshold of 290K has been widely utilized in previous research, as it corresponds to the brightness temperature typically observed at cloud tops near 1 km above the surface [45].

The higher threshold of 277K has been computed based on the average temperature of lower clouds which have cloud tops near 3km. By assuming a mean adiabatic lapse rate of about 6.5K per kilometer, it was calculated that the average temperature at 3 km altitude would be approximately 277K, starting from the 290K observed at 1 km above the surface.

Furthermore, to remove the bias that high clouds will produce, days where the 25th percentile of brightness temperatures within any satellite image is lower than 285K are discarded [45].

All relevant data and codes are available on https://github.com/Gheylla/thesis_project.

4.3.3 Day-to-day variability

In order to assess the presence of day-to-day variability in the simulated organization patterns, a similar approach to the one in Narenpitak et al. [46] is used.

Herein it is observed that from February 2nd 2020 to February 3rd 2020 there is a transition in the cloud patterns from sugar to flowers. Using these specific days, low cloud cover snapshots of the HARMONIE experiments are visually compared to the observational snapshots. Herefrom it can be concluded whether HARMONIE can simulate the transition from fine to larger cloud structures.

5 Results & Discussion

The results are divided into two main parts. The primary section focuses on cloud behavior, where the results of the computed cloud metrics are examined, herein the differences between the various experiments are discussed. The section after aims to address and present the various factors behind the observed differences.

Due to the significant emphasis of previous research on the diurnal cycle of cloud organization, only the diurnal cycle of the cloud organization metrics are illustrated below. The complete time series can be found in Appendix A.

5.1 Cloud Behaviour

5.1.1 Low cloud cover

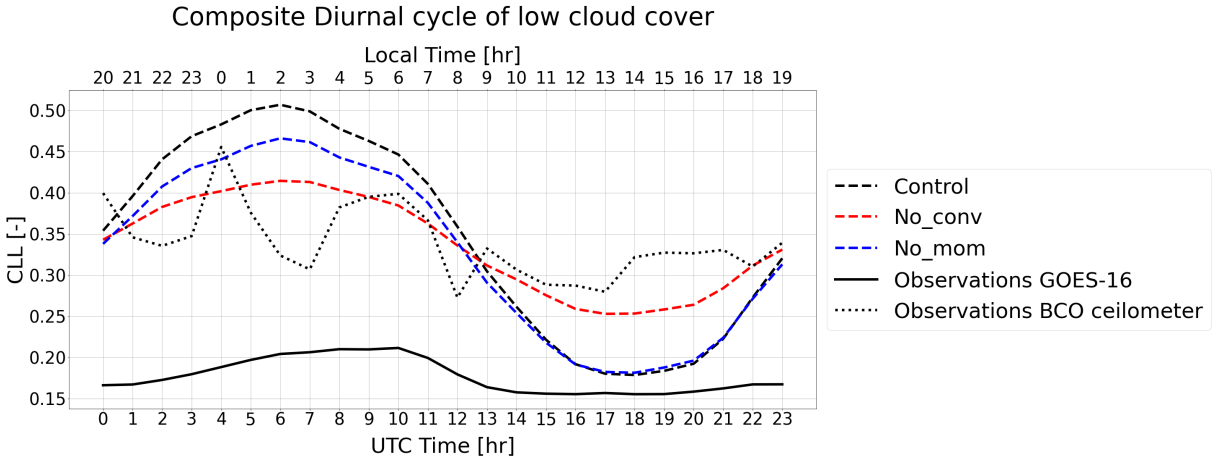

Figure 11: Composite Diurnal Cycle of Low Cloud Cover Computed With the Cloud Organization Metric Algorithm.

The first aspect that stands out from the diurnal cycle of cloud cover, Fig. 11, is the notable difference between the observed GOES-16 results and the simulated values. While the observations present a mean cloud cover of approximately 18 %, the 'control', 'no_conv', and 'no_mom' experiments exhibit a nearly twofold increase in mean cloud cover of approximately 35%, 34% and 33%, respectively. According to Jiménez, GOES-16 has a limited ability to detect low clouds. Resulting in the differences between the observations and the HARMONIE experimental outputs being attributed to the missdetection of low clouds by the satellite [47].

Although the GOES-16 results deviate from the experimental outputs, they are in line with what has already been presented in literature, see Vial, Vogel, and Schulz [28]. Herein the same satellite data from GOES-16 over the tropical Atlantic ocean near Barbados was utilized. The results show the same diurnal pattern. Herein it is also noted that the lower resolution of GOES-16 ABI prevents the detection of the smallest clouds and that the BCO radar ceilometer is much more sensitive to the low-level cumuli compared to the GOES-16 ABI infrared channel [28].

By comparing the HARMONIE experimental outputs with cloud cover measurements from the ceilometer located at the BCO, which is more accurate at measuring low clouds, it becomes evident that there is a significant difference in cloud cover measurements methods. From this comparison it is evident that HARMONIE is able to reproduce the observed cloud cover to some degree. Specifically the 'no_conv' experiment exhibits a more close relation to the ceilometer measurements. Both the experiment and the ceilometer observations produce a mean cloud

cover of approximately 34% .

There is a clear diurnal cycle present in the experimental outputs. Producing a minimum cloud cover during the afternoon [LT] and maximum during the night [LT]. Vial, Vogel, and Schulz have observed a similar pattern of cloud cover in the observations, which indicate that the HARMONIE experiments are able to reproduce the diurnal cycle and phase of cloud cover correctly.

Looking closely at the inter-experimental differences, 'no_conv' has a less pronounced diurnality compared to the other two experiments, producing the least cloud cover during the night [LT] but the most clouds during the day [LT]. This signals to a decreased variability in the types of clouds produced compared to the other experiments. Moreover, during the night it can be observed that all three experiments have differing cloud cover amounts, whereas during daytime 'control' and 'no_mom' have similar values. This indicates that the impact of momentum mixing on cloud cover is reduced when there is no incoming solar radiation.

Besides the studying the diurnal cycle of cloud cover researchers have also studied the diurnal cycle of the cloud population. According to Vial et al. there is clear diurnal cycle in cloud population in the trade wind region, consisting of shallow clouds visible during daytime and deeper clouds present during nighttime [29, 30]. These variations are likely driven by variations in the intensity of shallow convection and reflect the strength of cloud sensitivity to convective mass flux [30]. To investigate whether HARMONIE is able to produce this daily variation, the composite diurnal cycles of cloud fraction are presented in figures 12, 13 and 14.

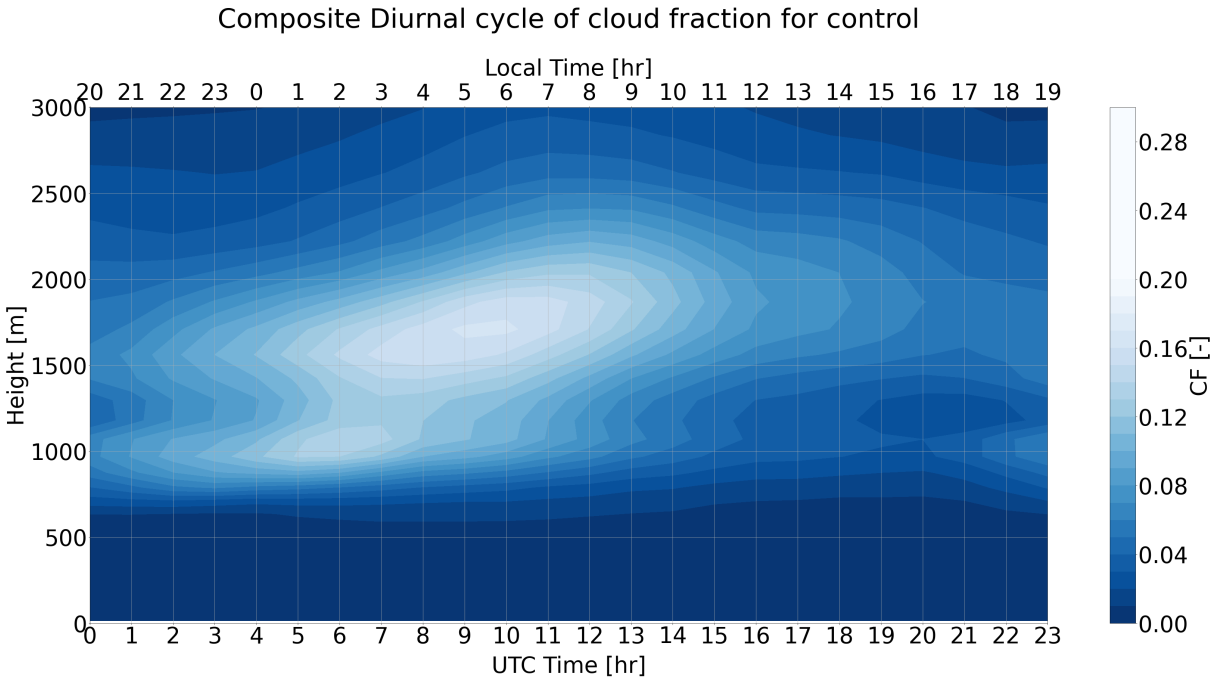

Figure 12: Composite Diurnal Cycle of Cloud Fraction From the HARMONIE Model Output for the Control Experiment.

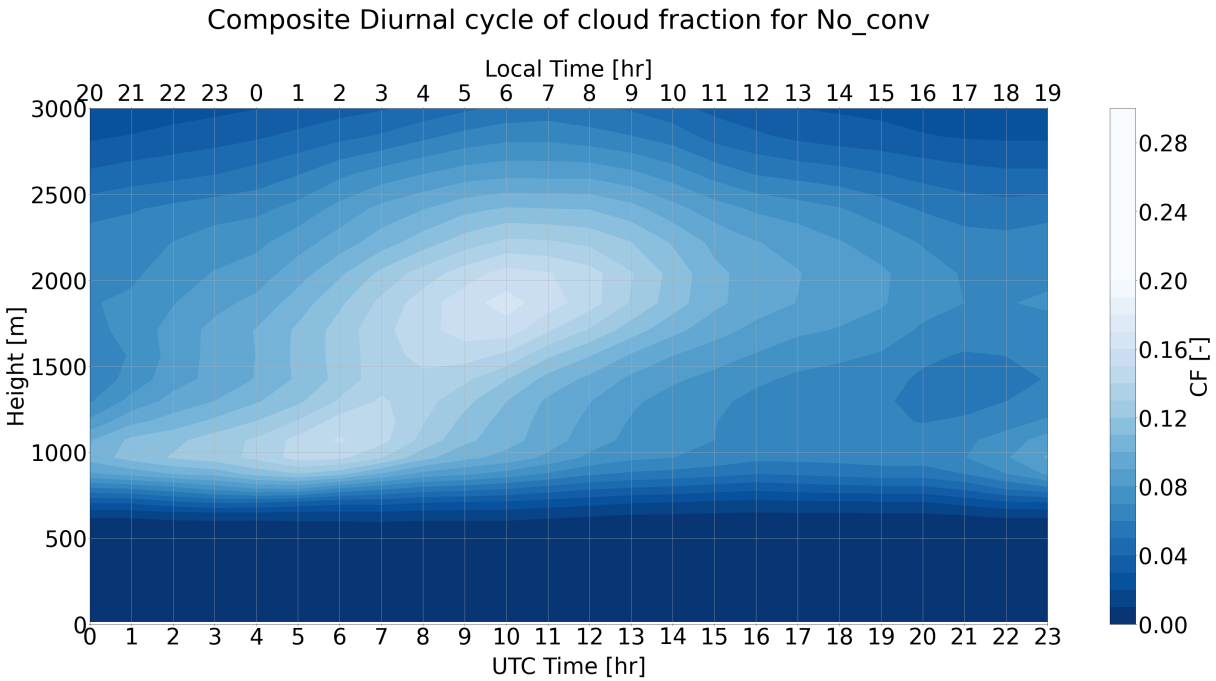

Figure 13: Composite Diurnal Cycle of Cloud Fraction From the HARMONIE Model Output for the No_conv Experiment.

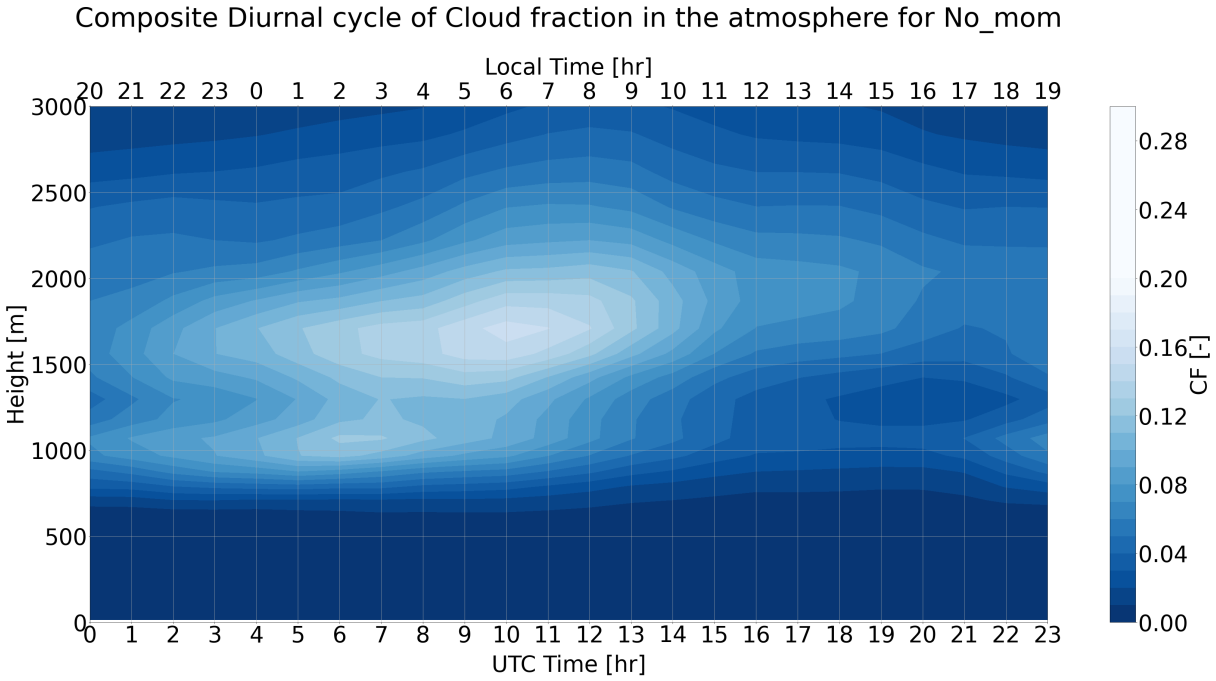

Figure 14: Composite Diurnal Cycle of Cloud Fraction From the HARMONIE Model Output for the No_mom Experiment.

In general there is a noticeable daily cycle present within the HARMONIE experiments. It can be seen that the clouds are the most shallow during sunset and at night [LT] and deepen reaching a maximum depth during the early morning, right before sunrise [LT]. These results align with the observations as discussed and presented by Vial et al. [30] and illustrate the ability of HARMONIE to qualitatively simulate the observed diurnal pattern in cloud population. Furthermore from these figures it is illustrated that 'no_conv' has the ability to produce deeper

clouds compared to the other experiments, this is further illustrated in Figure 15.

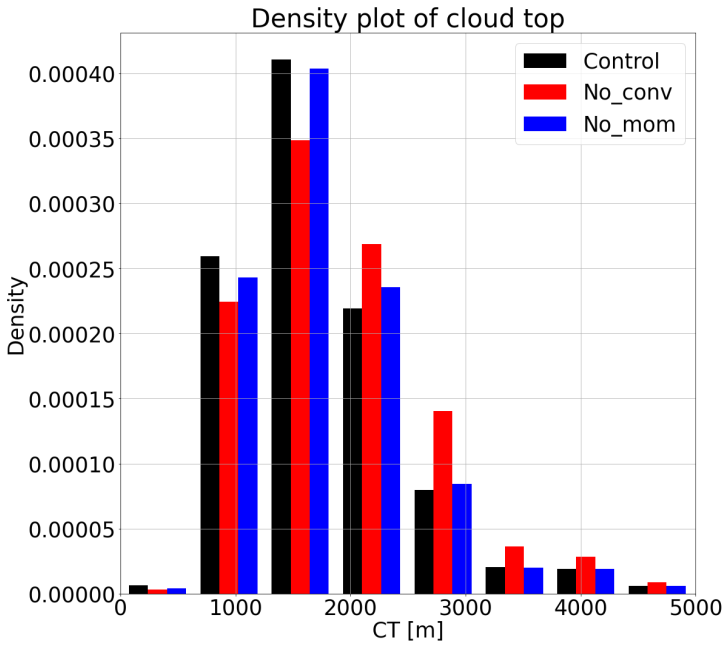

Figure 15: Density Plot of Cloud Top

The data presented in the figure shows that the 'no_conv' experiment contains more clouds with cloud tops ≥ 2000m, confirming the validity that the 'no_conv' experiment produces deeper clouds.

5.1.2 Size of voids

In addition to examining areas covered by clouds, it is also interesting to look at areas with no clouds, Fig. 16.

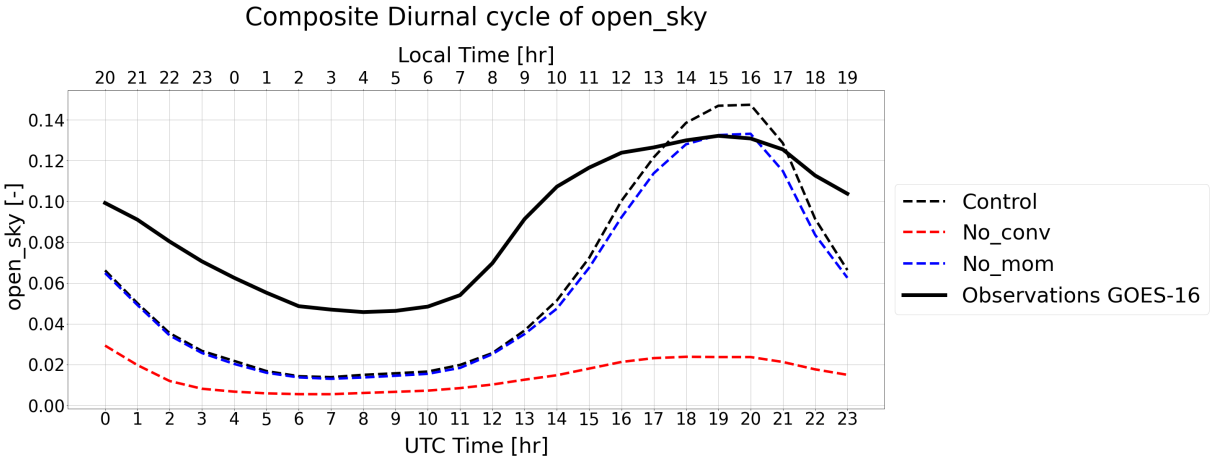

Figure 16: Composite Diurnal Cycle of Open Sky Computed With the Cloud Organization Metric Algorithm.

In this case, open sky refers to the maximum measurable distance that lacks any cloud cover [27]. When comparing Figures 11 and 16 with each other it can be seen that the cycle of diurnality of the voids is opposite to that of cloud cover. Denoting that during the night there is more

cloud cover with small empty spaces and during the day there is less cloud cover with larger cloud free areas. The absence of variation in the diurnal cycle of the open sky for 'no_conv' supports the notion that this particular experiment generates consistent cloud types throughout the entire day with little variation. The results also reveal that the diurnal pattern observed in the observations is partially captured in the 'control' and 'no_mom', although there are still noticeable variations in the values.

Initial observations of cloud cover and open sky suggest that there might be a correlation between the two variables. To delve deeper into these connections, the correlations between these metrics are presented in Figure 17.

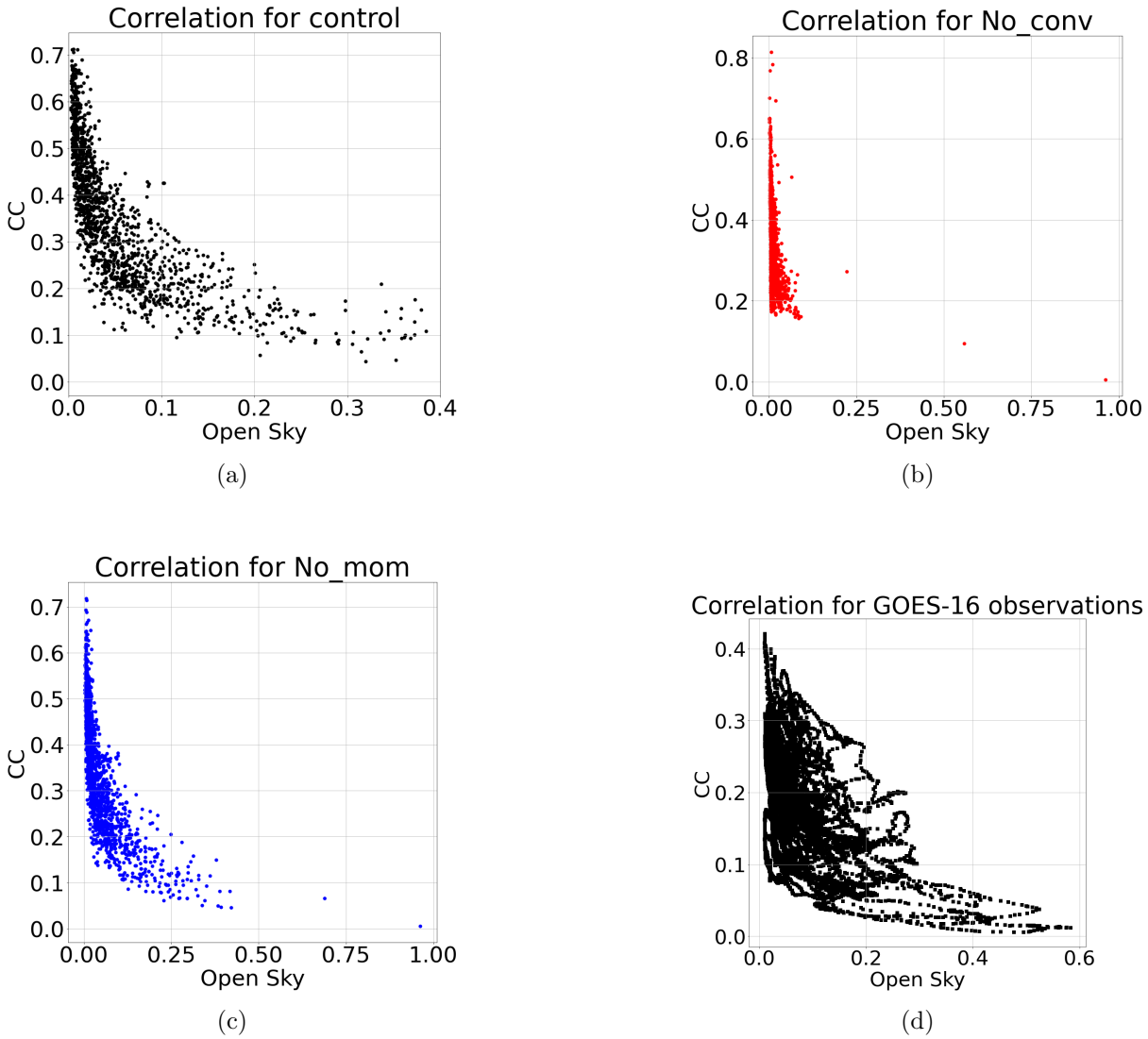

Figure 17: Correlation of Cloud Cover and Open Sky for the 'Control' (a), the 'No_conv' (b), 'No_mom' (c) and GOES-16 Observations (d).

From the results it is evident that there exists a negative (exponential) correlation between the open sky and the cloud cover. When cloud cover is large, the maximum size of the voids are small and vice versa. It is evident that the correlation is less prominent in the 'no_conv' experiment. In this experiment the open sky is unaffected by fluctuations in cloud cover. This indicates that despite changes in cloud cover, whether it involves an increase in the number or size of clouds, the overall arrangement within the field remains largely unchanged.

5.1.3 Number of cloud entities

When analyzing the cloud cover and open sky it is not possible to state what type of clouds and organization is being produced by the experiments. To aid in this analysis is the number of objects is presented in Figure 18.

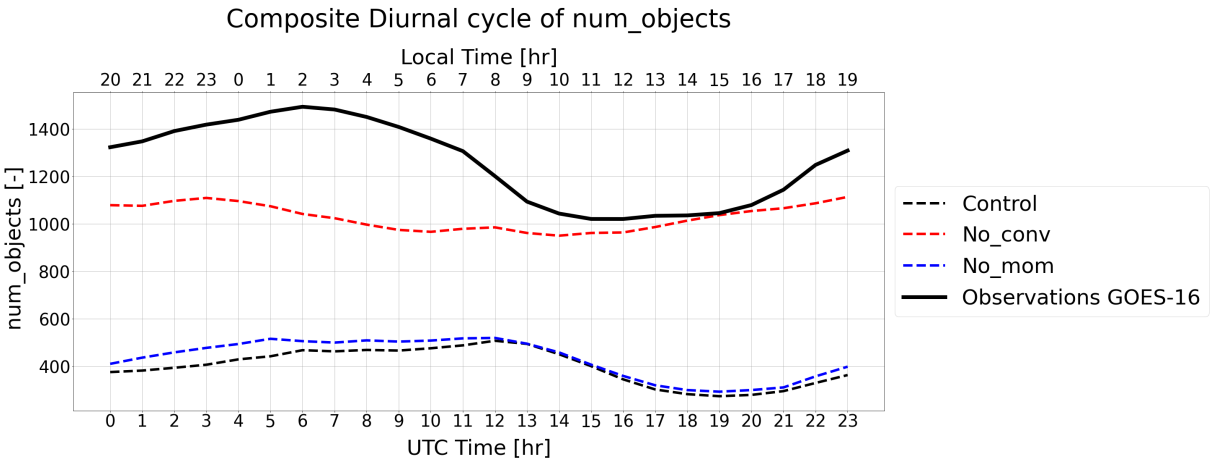

Figure 18: Composite Diurnal Cycle of Number of Objects Computed With the Cloud Organization Metric Algorithm.

Among the experiments, only the 'no_conv' experiment exhibits a modest ability to replicate the observed number of objects. However, it fails to reproduce the observed diurnal cycle. From the results it can be deduced that 'no_conv' produces significantly more cloud entities compared to the other experiments throughout the whole day. A visual representation of the difference can be seen in Figure 19.

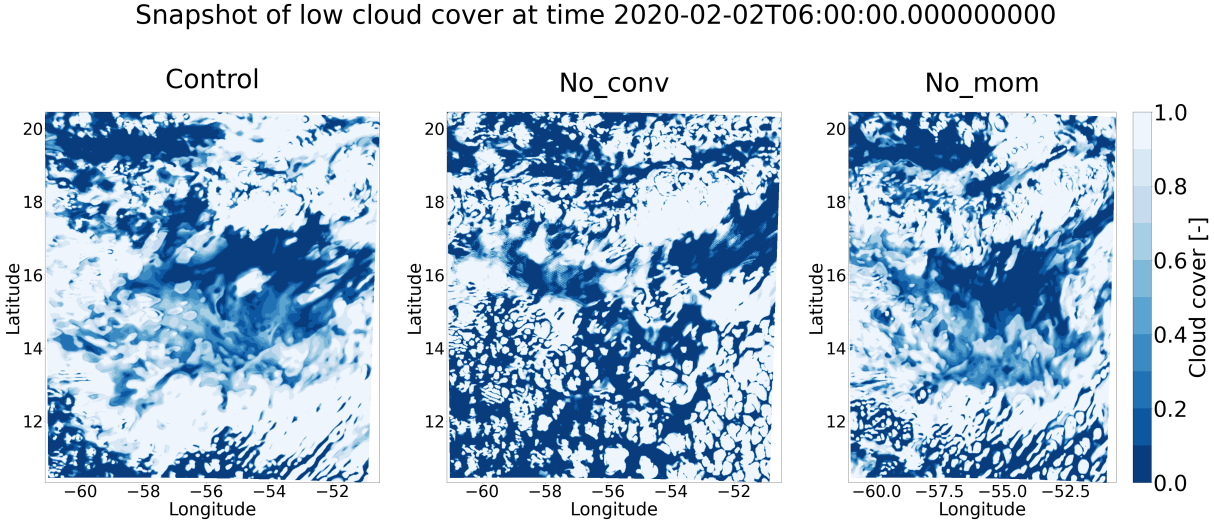

Figure 19: HARMONIE Snapshot of Low Cloud Cover at Time 2020-02-02T06:00:00 for 'Control' (Left Panel), 'No_conv' (Middle Panel), 'No_mom' (Right Panel).

Visually it is clear that the large cloud clusters that are present in the 'control' experiment are broken up into smaller cloud entities within 'no_conv'. Furthermore because the 'no_conv' experiment shows lack of variability in all of the composite diurnal cycles of the computed metrics it suggests that these small cloud formations are consistently generated. Lastly, it can be seen

that there is not significant difference between the 'control' and the 'no_mom' experiment. Even though the 'no_mom' experiment generates a slightly higher number of cloud entities, it continues to produce the same type of cloud formations as observed in the 'control' experiment.

5.1.4 Size of cloud entities

Further insights on the cloud types and organization can become more clear by looking at the various sizes of the clouds produced by each experiment. Figures 20a, 20b and 20c present the mean length scale, perimeter length and maximum length scale respectively.

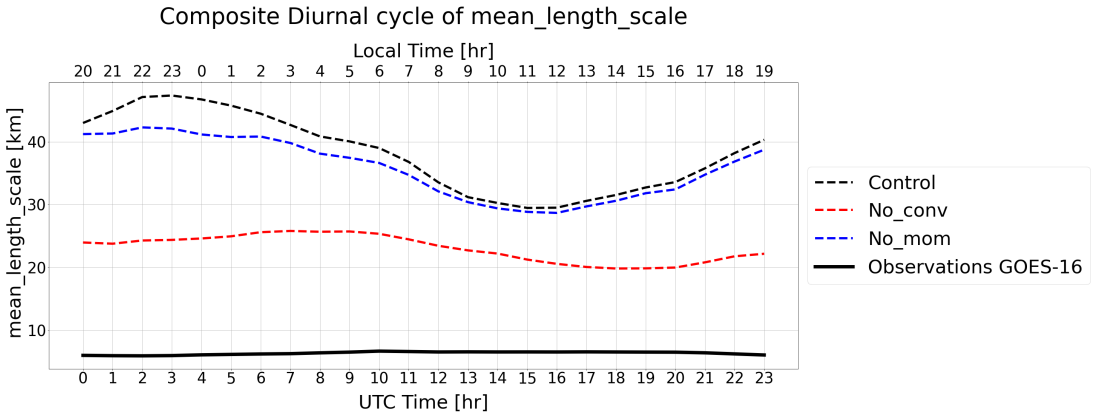

(a) Composite Diurnal Cycle of Mean Length Scale Computed With the Cloud Organization Metric Algorithm.

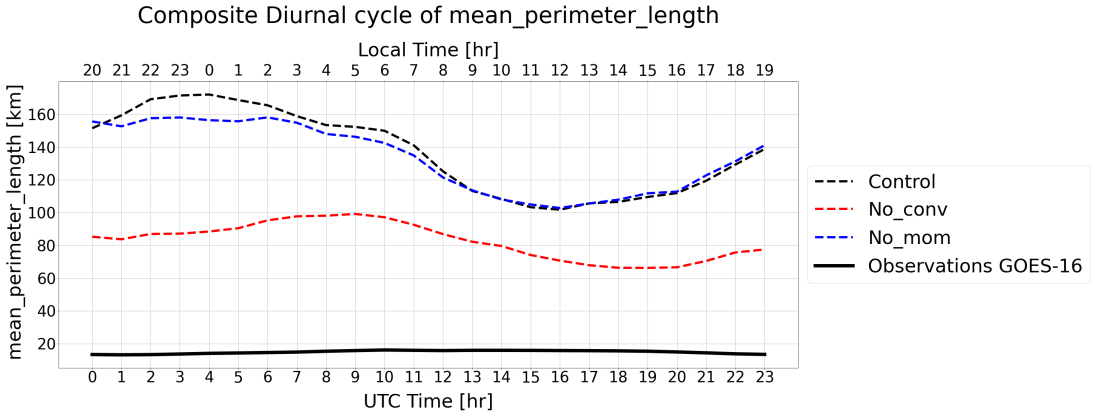

(b) Composite Diurnal Cycle of Mean Perimeter Length Computed With the Cloud Organization Metric Algorithm.

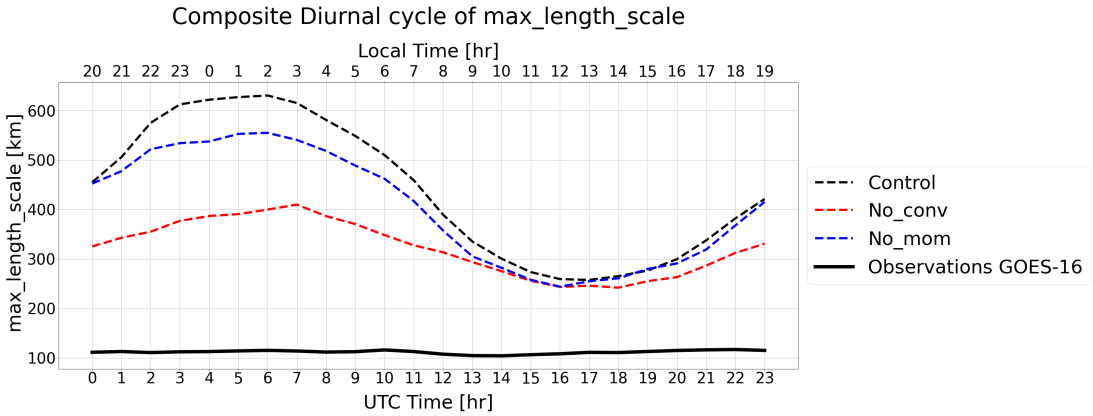

(c) Composite Diurnal Cycle of Maximum Length Scale Computed With the Cloud Organization Metric Algorithm.

Figure 20: Composite diurnal cycle of mean length scale, mean perimeter length and maximum length scale.

From the Figures it is evident that there is little to no diurnality in the observational data. The observation results of the mean length scale and mean perimeter length show similar diurnality with a very small increase in size of the cloud entities in the early morning.

For the HARMONIE experiments there is a clear diurnal pattern, that is the explicitly visible for 'control' and 'no_mom'. There are larger cloud structures present during the night [LT] while smaller clouds are present during daytime [LT]. Furthermore, it can also be seen that the differences between these experiments are larger during the night [LT] than during daytime [LT], enforcing the notion that momentum mixing again has more effect on the types of clouds and their size mostly during the night [LT]. The diurnal cycle in the various length scales is less pronounced for 'no_conv', elucidating the fact that this experiment has little variation in the clouds produced.

Integrating the results of cloud cover, number of objects and sizes of clouds entities altogether, it can be concluded that the diurnality of cloud cover for the 'control' and the 'no_mom' experiments is primarily influenced by the sizes of the cloud entities, whereas for 'no_conv' it is dominated by the number of clouds that are generated by the model. All of the experiments produce a maximum cloud cover during the night [LT], and a minimum during the day [LT]. The 'control' and 'no_mom' produce the least number of cloud entities during the whole diurnal cycle but have significant diurnal cycle in the sizes of the cloud objects producing the largest clouds during the night [LT] and the smallest during the day [LT]. On the other hand 'no_conv' does not have the ability to produce differing cloud sizes throughout the diurnal cycle. This experiment produces the same sizes of clouds, at a much higher concentration compared to the other experiments, resulting in its diurnal pattern being dominated by the amount of clouds it produces.

5.1.5 Organization index

Analyzing the metrics altogether gives a subtle insight into what the cloud organization within the cloud field is.

Summarizing; The 'control' experiment produces more cloud objects which are overall larger in size and has the smallest voids at night. Resulting in a more clustered pattern during the night compared to daytime. For the 'no_mom' experiment the same pattern is expected, while for

the 'no_conv' experiment it can be deduced that during the day and night the cloud entities are small, with a slight increase in size during the night, and high in numbers concentration. As a result of this it is expected that the type of organization is rather regular throughout the whole day. One way to objectively illustrate this is by looking at the organization index as presented in Figure 21.

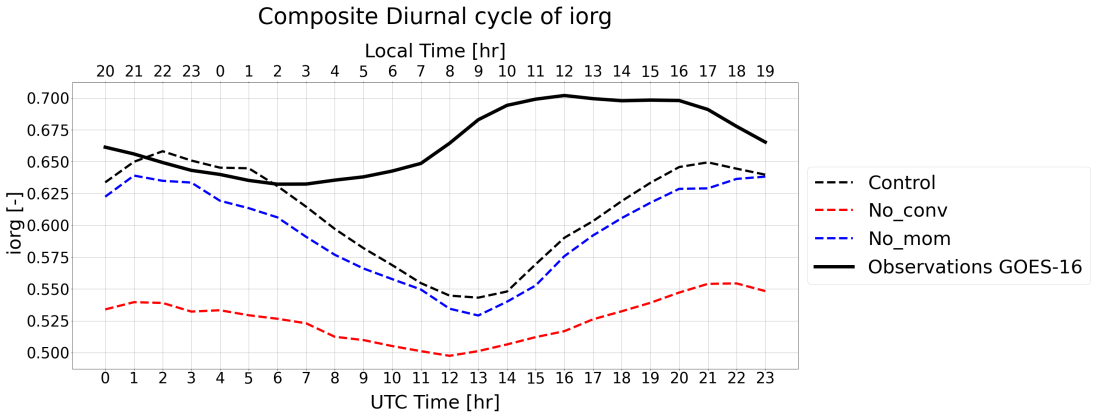

Figure 21: Composite Diurnal Cycle of Cloud Organization Index (Iorg) Computed With the Cloud Organization Metric Algorithm.

It is immediately clear that the experiments have a different cycle than what the observations show. At nighttime [LT] the observational values for Iorg are at a minimum and reach a maximum during the afternoon [LT]. On the contrary, all of the HARMONIE experiments exhibit an opposite cycle, producing high Iorg values during the night and afternoon and a minimum during the early morning [LT].

When comparing the observational diurnal cycle of Iorg with the ones produced by Large Eddy Simulations (LES), see Figure 22, a similar cycle can be observed between the two. Even though the values may not coincide it can be seen that the LES are able to produce a minimum during the night and achieve a maximum during the day.

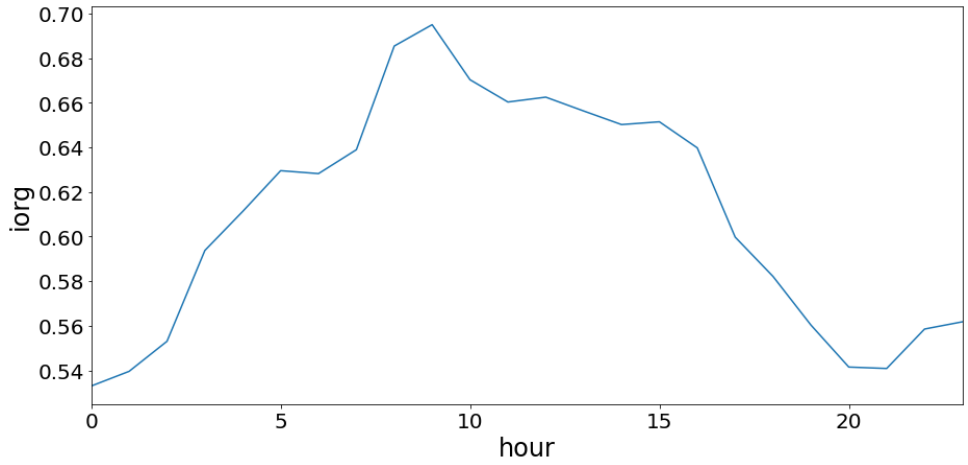

Figure 22: Composite Diurnal Cycle of Cloud Organization Index (Iorg) Computed from LES simulations produced by Alessandro Savazzi.

These LES are produced over a smaller domain and have a much finer spatial resolution compared to the HARMONIE experiments. The lack of fine-grained spatial resolution in the HARMONIE experiments might result in their inability to adequately capture the degree of organization.

Looking at the inter-experimental differences, both the 'control' and the 'no_mom' experiments have a more clustered pattern during the night [LT] which evolves to a more random cloud distribution during the early morning and going back to clusters in the afternoon [LT], as expected. For the 'no_conv' experiment the cycle of organization is not as pronounced as the other experiments. All values of Iorg are much closer to 0.5 during the whole day, reaching 0.5 during the early morning.

Eventhough a periodic cycle is visible for the 'control' as well as for the 'no_mom' experiment, all values of Iorg are above 0.5. According to the definition, this implies that these experiments are generating clusters throughout the entire day. For the 'no_conv' experiment the values of Iorg are much closer to 0.5, denoting randomly distributed clouds. Based on this observation, it can be inferred that the 'no_conv' exhibits less organization in comparison to the other experiments.

5.2 What is the cause for the various disparities?

Upon examining the various results of the computed cloud metrics, it is crucial to determine the cause for the presented differences. From the analysis of the cloud organization metrics it has been revealed that the 'no_conv' experiment exhibits the least amount of cloud cover during the night [LT] and the most during the day [LT] in comparison to the other experiments. Furthermore, this experiment generates a significant number of smaller-sized cloud entities and displays the least variability in terms of diurnal patterns. Moreover, it has also been shown that the 'no_mom' experiment exhibits a more pronounced influence during the night [LT] than during the day [LT].

Past research has shown that the daily cycle of cumulus clouds present in the North Atlantic trade-wind region is not sensitive to changes in the sea surface temperature along with breezes from sea to land, but can be mostly attributed to the increase in surface winds and buoyancy fluxes during the night [28, 29, 48–50]. According to the findings of Vial et al., model configurations play a crucial role in the cloud production and the daily variation [30]. Differing contributions of convective and turbulent transports to the total subgrid-scale transport can lead to differences in simulated cloud fraction and cloud depth [30]. These findings serve as the motivation for investigating the disparities between the HARMONIE experiments.

5.2.1 Water Balance

Cloud formation is closely related to the availability of water within the atmosphere. As the air becomes saturated with water vapor due to factors like evaporation from water bodies, transpiration from plants, and moisture influx from precipitation, it reaches a point where the air can no longer hold all the moisture. This leads to condensation, which water vapor transforms into liquid water droplets or ice crystals, forming clouds.

The results show that the various HARMONIE experiments have different cloud behaviours. To determine the cause for these differences, it is necessary to examine the availability of moisture required for cloud formation within all of the HARMONIE experiments. Table 2 shows an overview of the precipitation, evaporation and the resulting water balance.

Table 2: Overview of the Mean Precipitation (P), Mean Evaporation (E) and the Resulting Water Balance (E-P) for All of the HARMONIE Experiments.

	Experiment Name	**Mean Precipitation [mm/hr]**	**Mean Evaporation [mm/hr]**	**Water Balance (E - P)**
1	Control	0.0396	0.3179	0.2784
2	No_conv	0.0460	0.2944	0.2484
3	No_mom	0.0330	0.3128	0.2798

Although the reduced moisture availability could explain the slightly lower cloud cover compared to the 'control' experiment, it contradicts the findings that indicate the number of cloud entities is practically doubled compared to the 'control' and 'no_mom'.

5.2.2 CAPE

As the variations between the different experiments cannot be completely attributed to the water balance, further investigation into the atmospheric physics of each experiment is necessary to gain a deeper understanding of the differences.

As already briefly discussed and presented in Section 5.1 it is anticipated that by disabling shallow convective parametrization, instability is able to build up reaching significant values. An objective way to establish this is by analyzing the measure of instability of the atmosphere, also referred to as the Convective Available Potential Energy (CAPE). By looking at the probability density function and the composite diurnal cycle of CAPE, it can be possible to determine whether and how the instability varies across the various experiments. Figure 23 & 24 give the density plot and the composite diurnal cycle of CAPE respectively.

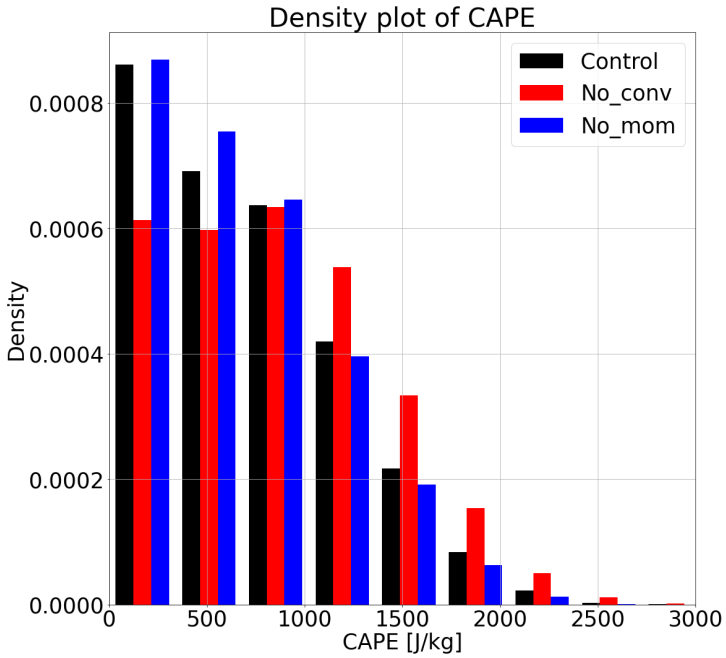

Figure 23: Density Plot of Convective Available Potential Energy (CAPE) for all of the HARMONIE experiments.

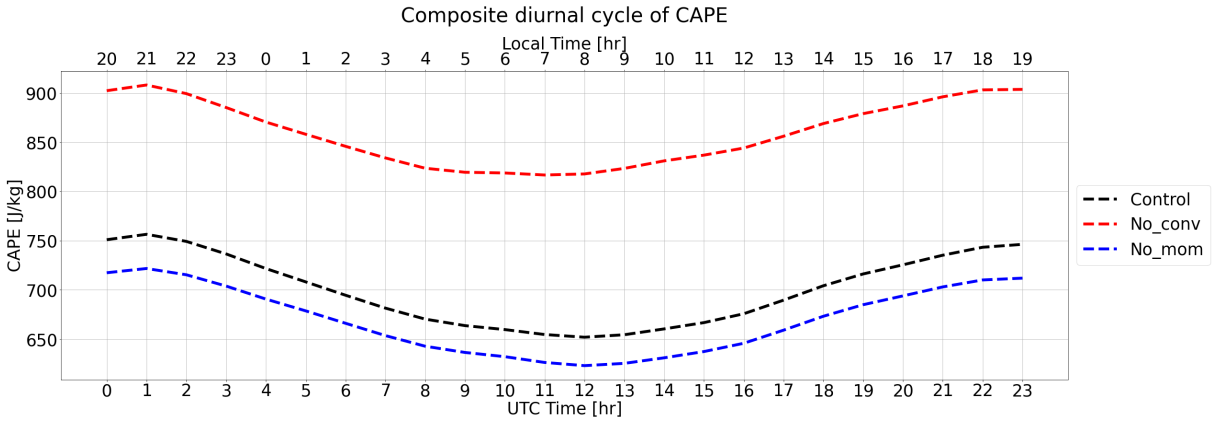

Figure 24: Composite Diurnal Cycle of Convective Available Potential Energy (CAPE) for all of the HARMONIE experiments.

From Figure 23 it is evident that the 'control' and the 'no_mom' experiments have much more instances of lower CAPE compared to the 'no_conv' experiment. 'No_conv' has a heavier tail, which indicates that it contains more instances of higher CAPE values. From the composite diurnal cycle it is also evident that the 'no_conv' experiment continuously contains more instability, see Fig. 24. This confirms the hypothesis that instability is able to build up within the 'no_conv' experiment producing significant energy for potential updrafts.

When shallow convective parametrization is **disabled**, instability is able to accumulate within the model. As it accumulates and reaches a significant level, resolved convection will remove this instability. Once resolved convection is present and working within the model, the concerning gridbox will always contain sufficient liquid water or ice to make cloud formation possible, leading to the production of a completely cloudy gridbox. However, it will not be large areas of clouds. This occurs across the entire model domain, resulting in small cloud patches distributed across the entire area.

On the other hand, the objective of having parametrized shallow convection within the model is to eliminate instability through shallow convective mixing. With parametrized shallow convection **enabled** within the model, instability is immediately removed and will not accumulate at the same extent as when shallow convective parametrization is disabled. This convection parametrization is present over larger areas of the model and is able to produce larger areas of clouds.

Because CAPE does not accumulate as much and as fast within 'control' and the 'no_mom' experiments as compared to 'no_conv', the resolved convection is less dominant within these models. Consequently the model gridboxes have the ability to contain more fractional cloudiness whereas when shallow convective parametrization is disabled the model functions more as an all or nothing scheme. Figure 9 provides supporting evidence of this, showing that the 'no_conv' experiment has much more instances of no cloud cover (cc = 0) and completely cloudy (cc = 1) pixels compared to the other experiments. Take into consideration that the 'no_conv' experiment still produces fractional cloudiness within the pixels because the cloud scheme is still enabled. The cloud scheme estimates the sub-grid cloud fraction and the condensed water by assuming a distribution of temperature and humidity and determining the cloud cover as the fraction of the distribution that is above saturation [33].

The continuous accumulation of CAPE within the 'no_conv experiment is the reason for the continuous production of small clouds throughout the entire cloud field, as presented in section 5.1.3

5.2.3 Up- and downdraft strengths

CAPE provides an estimation of the updraft strengths within the atmosphere. Because there are more instances of high CAPE within the 'no_conv' experiment it is generally expected that this experiment would contain more extremes, and consequently produce stronger up- and downdrafts. This is objectively illustrated in Figure 25.

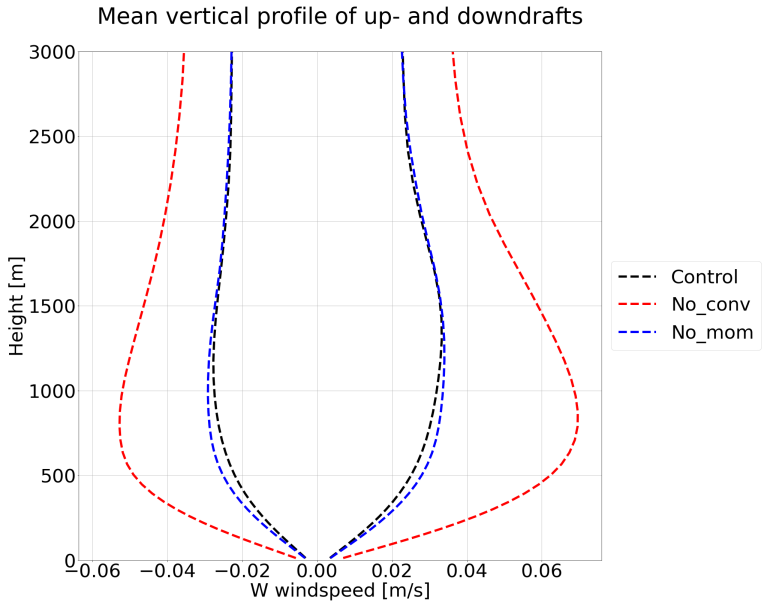

Figure 25: Mean Vertical Profile of Up- and Downdrafts (W-Wind speed) for all of the HARMONIE Experiments.

The Figure clearly illustrates how the 'no_conv' experiment produces stronger up- and downdrafts, which is in line with what is expected. What can also be seen is that the 'no_mom' experiment also has a slight increase in up- and downdrafts compared to the 'control'. From the density plot of CAPE, Fig. 23, it can be observed that 'no_mom' has slightly more instances of CAPE values around 0 - 1000 J/kg compared to the 'control'. This may be the reason for the slight increase in up- and downdraft strengths between 'no_mom' and 'control'.

The stronger updrafts can be explained by the accumulation of instability, as already discussed. However, updrafts can also be enhanced due to the presence of condensed water within the region. The condensation of water vapor releases latent heat into the atmosphere, causing the parcel of air to become warmer than its surroundings. This, in turn, amplifies buoyancy and generates more powerful updrafts. The amount of water present within the atmosphere is visually depicted in Figure 26.

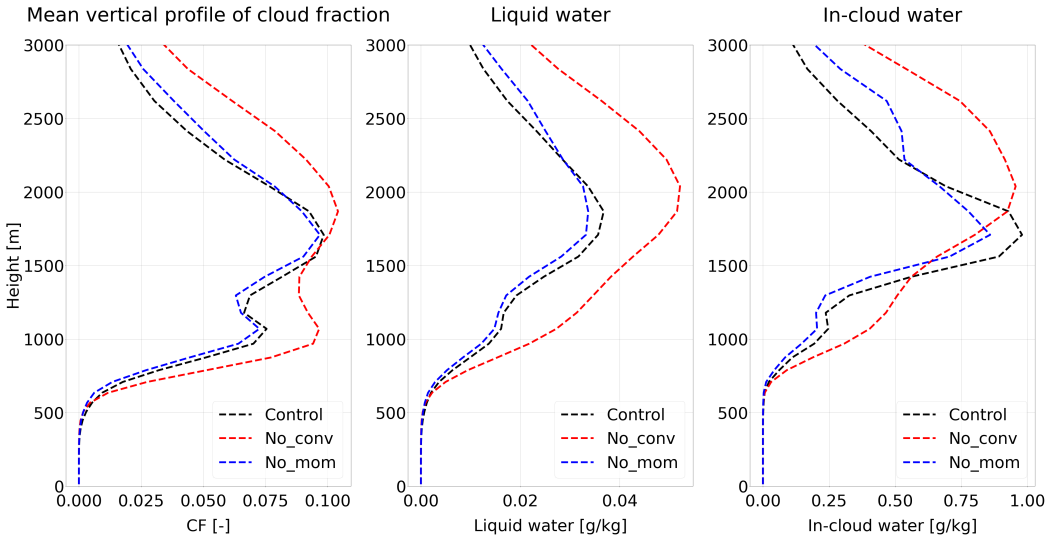

Figure 26: Mean Vertical Profile of Cloud Fraction (CF) (Left Panel), Total Liquid Water (Middle Panel), In-Cloud Water (Right Panel) for all of the HARMONIE Experiments.

The 'no_conv' experiment overall contains more liquid water throughout the whole vertical extent. Hence, it can be inferred that the greater amount of liquid water is an additional factor contributing to the stronger updrafts observed in this experiment.

One aspect that remains unaddressed is if whether the overall greater amount in total liquid water is due to the overall increase in clouds or if it is due to the clouds becoming more saturated with water. By analysing Figure 26, right panel, it can be seen that the 'no_conv' experiment contains the most in-cloud water between 600m-1400m and from approximately 1900 m upwards. Moreover, it exhibits the highest average in-cloud water content, reaching a total of 0.15 g/kg. In contrast, both the 'control' and 'no_mom' experiments yield means of approximately 0.11 g/kg and 0.10 g/kg, respectively. This indicates that the total liquid water of 'no_conv' is mostly dominated by the amount of water that is present within the clouds. The clouds have become more saturated with water. Only within the range of 1400m-1900m the quantity of total water within the 'no_conv' experiment is dominated by the amount of clouds present in this experiment.

5.2.4 Precipitation

The presence of water within clouds has a direct relationship with precipitation. As clouds become more saturated with water, the water droplets within them have the potential to increase in size and ultimately lead to precipitation. Upon examination of the vertical distribution of in-cloud water, as depicted in Figure 26, it is probable that the 'no_conv' experiment would yield the highest precipitation, followed by the 'control' experiment. Conversely, the 'no_mom' experiment is expected to generate the least amount of precipitation.

To further investigate the ability of precipitation production of each experiment the diurnal cycle of precipitation is depicted in Figure 27.

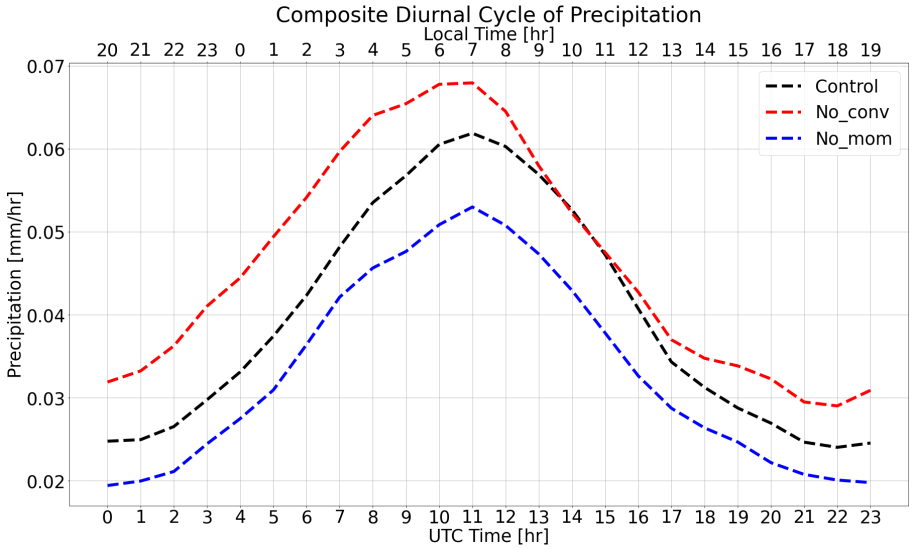

Figure 27: Composite Diurnal Cycle of Precipitation for all of the HARMONIE Experiments.

As expected, it is clear that the 'no_conv' experiment precipitates the most overall, followed by the 'control' and lastly the 'no_mom' experiment.

In addition to the water availability, the configurations of the model also play a role in determining the precipitation production. Shallow convective parametrization is able to produce

precipitation but often weakens this production. For significant amounts of precipitation it is more favourable to rely only on resolved convection. This also explains why the 'no_conv' experiment has the most amount of precipitation compared to the other experiments. For the 'control' where shallow convection is enabled, water vapor can be transported to the free troposphere making the convective boundary layer drier, resulting in less precipitation compared to the 'no_conv' experiment.

Past research has also observed a diurnal cycle in precipitation. Here from a nighttime/early morning maximum in precipitation and a minimum during the afternoon was observed [30, 51]. This diurnal cycle can also be seen the various HARMONIE experiments, see Fig. 27, which indicates that HARMONIE is qualitatively able to reproduce the observed pattern in precipitation.

5.2.5 Humidity

It has been shown that the 'no_conv' experiment demonstrates more robust updrafts and deeper convection. This indicates that despite the absence of consistent low-level mixing in this model, during episodes of deep convection, moisture from the surface is transported to higher altitudes in the atmosphere.

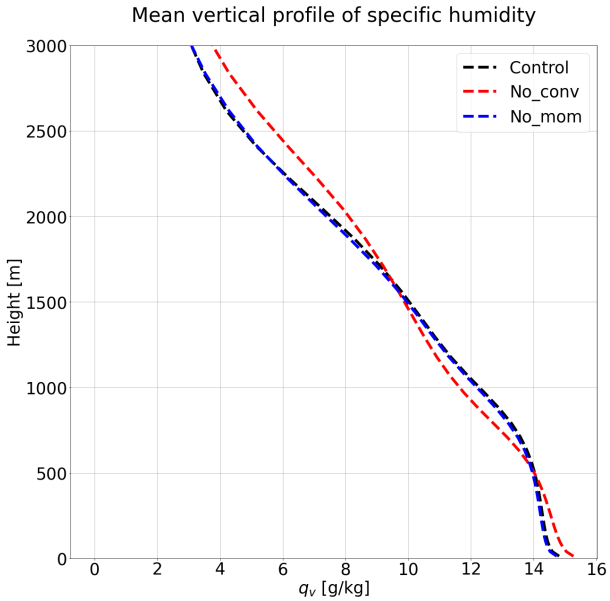

Figure 28: Mean vertical profile of specific humidity.

The average vertical profile in Figure 28 reveals that the 'control' and the 'no_mom' experiments exhibit greater mixing in the lower parts of the atmosphere. This again is expected as the presence of shallow convection helps to move humid air to levels higher up in the atmosphere, producing a more homogeneous profile of humidity through the continuous mixing. This profile also indicates that there are instances of deeper convection present within 'no_conv'. These are able to bring moisture from near the surface to levels higher up in the convective boundary layer resulting in increased humidity from approximately 1500m upward compared to the other experiments.

Moreover, the influence of momentum mixing from UV mix on atmospheric humidity is not significant, as there is only a minor decrease in humidity. Therefore, it can be inferred that shallow convection primarily drives the mixing of humidity within the atmosphere.

5.2.6 Buoyancy & Winds

According to Vial et al., the daily cycle in cloud formation and depth can be interpreted as a result of a nighttime increase in surface winds and buoyancy fluxes [30]. However, depending on the model, the relative contribution of convective and turbulent transports to the total subgrid-scale transport may differ, which can in turn lead to differences in simulated cloud fraction and cloud depth. Overall it can be seen that with an increase in mass flux, clouds are expected to deepen [30]. To determine the differences between the daily cycles of cloud fraction for the various HARMONIE experiments the vertical profiles of liquid water potential temperature flux are presented in Figure 29.

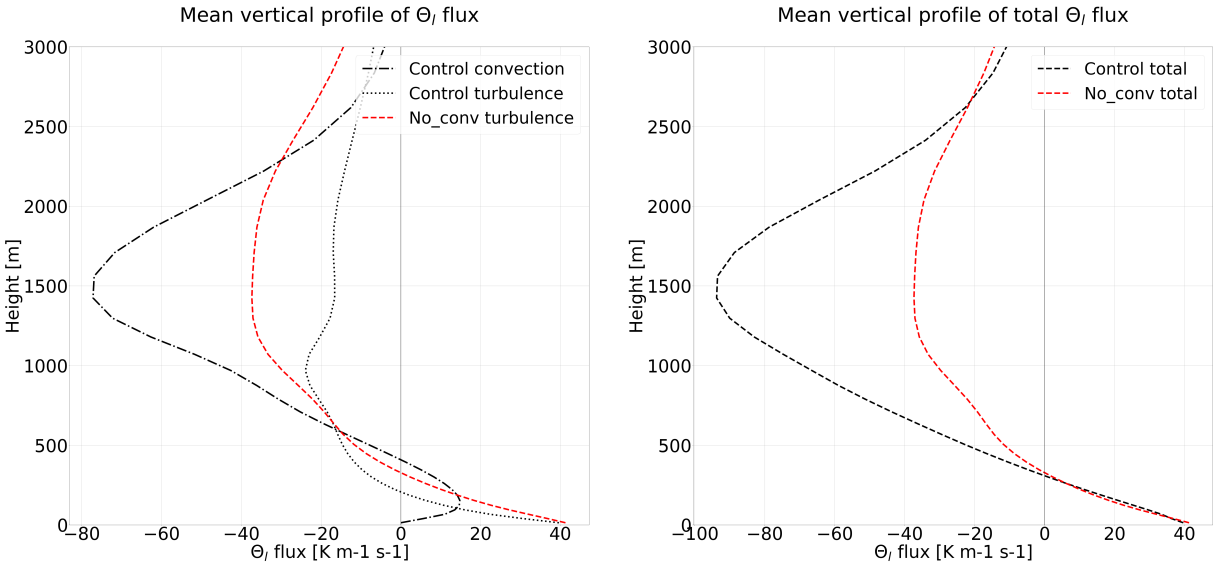

Figure 29: Mean Vertical Profile of Liquid Water Potential Temperature Flux (Θ_l flux).

From these profiles, valuable insights can be obtained regarding the strength of convection. The left panel divides the Θ_l flux into the contribution by turbulence and convection separately. Whereas the right panel shows the overall total flux.

In the analysis of the right panel, it is evident that both experiments exhibit a positive flux near the surface, specifically up to approximately 300m. This suggests the presence of upward movement of warm air in this region. Both experiments demonstrate a similar vertical profile and quantity of vertical flux in this particular area, indicating comparable values of vertical transport. However, upon closer examination of the individual contributions of convection and turbulence, left panel, it becomes apparent that the 'control' experiment shows a predominance of turbulence in the lower levels, transitioning to a dominance of convection as the altitude increases. In contrast, the total flux of Θ_l in the 'no_conv' experiment is only influenced by turbulence.

This transition from turbulence to convection and difference between the two experiments is expected. Turbulence is able to transport parcels within the lowest 200m of the atmosphere, while convection takes over to transport these parcels further upward. In the case of the 'no_conv' experiment, where shallow convection is disabled, the absence of convection-related contributions is compensated by turbulence. Consequently, turbulence takes on the entire workload and becomes the primary driving force behind the flux.

From 400m upward there is subsiding motion for both of the experiments. This suggests that the air parcels are descending rather than ascending, which is generally unfavorable for cloud

formation. The reduced magnitudes of subsidence can be seen as an additional indication for the higher cloud production observed in the 'no_conv' experiment.

Winds are an important aspect for the development of convection and clouds within the atmosphere. As Savazzi et al. presented in their paper, an accurate representation of winds is essential for better convective parametrizations. Based on these findings it is crucial to consider and analyze the the diurnal cycle of total winds as depicted in Figure 30.

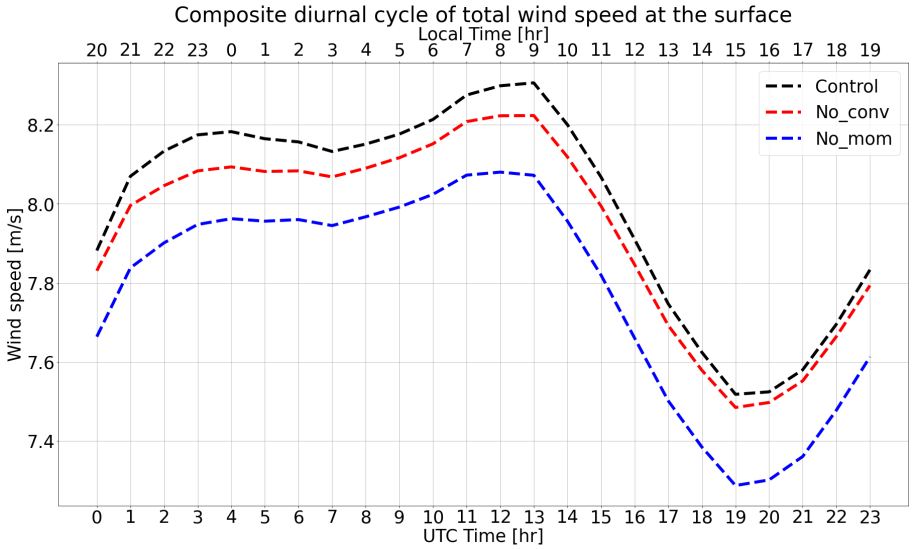

Figure 30: Composite Diurnal Cycle of Total Surface Wind speed for all of the HARMONIE Experiments.

The results show a clear diurnal pattern in total surface wind speed. The experiments show a pattern consisting of higher winds during the night and early morning [LT] and weaker winds during daytime [LT]. The same diurnal cycle can also be seen in observations as presented in the paper by Savazzi et al. [48], indicating that the HARMONIE experiments are able to reproduce the diurnal cycle in wind for the domain in question.

Although the experiments successfully capture the qualitative aspects of diurnal variability of total wind speed, they tend to overestimate the amplitude quantitatively. In the observations [48], the total wind speed ranges from approximately 9.5 m/s to 8.9 m/s, whereas the experiments exhibit an amplitude of approximately 1 m/s, which is nearly double the observed amplitude.

Looking at the inter-experimental differences, it can be seen that the 'no_mom' experiment displays the weakest surface winds overall. This outcome is expected since this experiment specifically disabled mixing caused by wind. This results in the inability of the experiment to bring stronger winds aloft down, producing weaker winds near the surface.

Surprisingly, the 'no_conv' experiment yields stronger winds in comparison to the 'no_mom' experiment. This is unexpected because the 'no_conv' experiment disables all types of mixing, consisting of temperature, momentum and moisture. It would be logical to assume that by disabling everything along with wind, the resulting winds would be even weaker. However, it appears that there are other mechanisms at play, exclusive to the complete removal of the shallow convection, which allow for some form of mixing to persist. One possibility could be that resolved convection is responsible for this phenomenon.

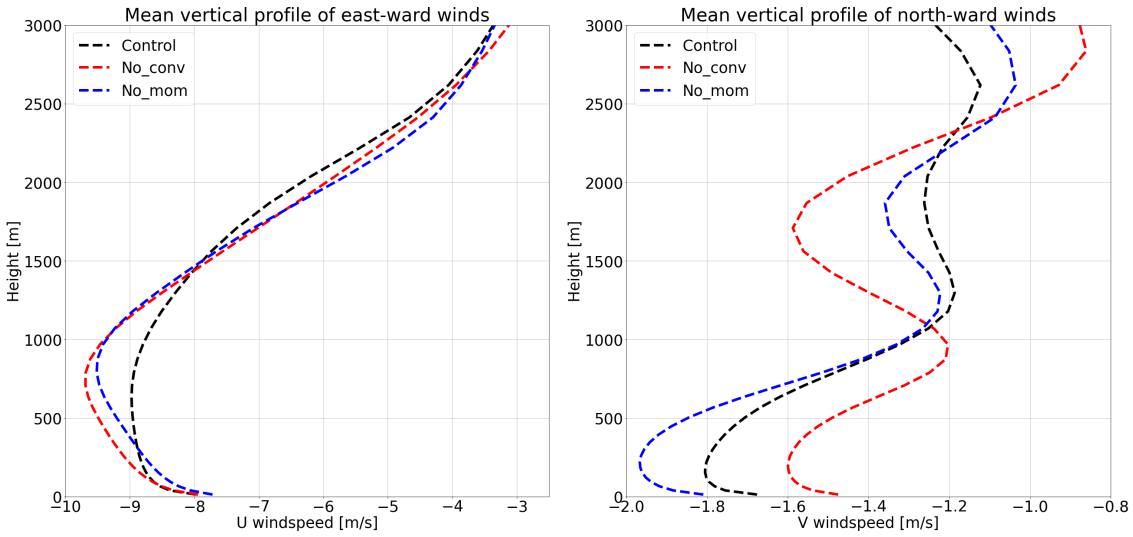

(a) (b)

Figure 31: Mean Vertical Profile of East-Ward (U) Winds (Left Panel) and North-Ward (V) Winds (Right Panel).

From the mean vertical profile of the eastward winds, Figure 31a, it is observed that the eastward winds are much more mixed in the lower atmospheric layers for the 'control' than the other experiments. This is expected as shallow convection and momentum mixing are both enabled in this experiment. As a result, this makes it possible for the downward transport of stronger winds from higher altitudes and the upward movement of weaker winds from the surface, creating a significantly more blended and mixed layer within the atmosphere, similar to figure 5.

Besides this, the wind speeds near the surface are the smallest for the 'no_mom' experiment. For the 'control' and the 'no_conv' experiment the wind speeds near the surface are the relatively similar, indicating that the presence of shallow convection scheme only influences the winds higher up in the atmosphere.

Finally, based on the east- and northward windspeed values, it is evident that the eastward component predominantly influences the overall magnitude of the total wind speed.

5.3 Visual organization

To determine whether HARMONIE is able to reproduce the day-to-day variability in cloud patterns, two days where the observations show a change in patterns are compared to the HARMONIE cloud field outputs. This method was conducted by Narenpitak et al., where cloud fields of model experiments were compared to observational cloud fields of days where there is a transition in cloud patterns. Herein it is observed that from February 2nd to February 3rd there is a transition in the cloud patterns from sugar to flowers.

The figures below are a snapshot of the cloud cover at times 02/02/2020 at 12:00 UTC, 02/02/2020 20:00 UTC, 03/02/2020 02:00 UTC and are chronologically arranged vertically, from top to bottom.

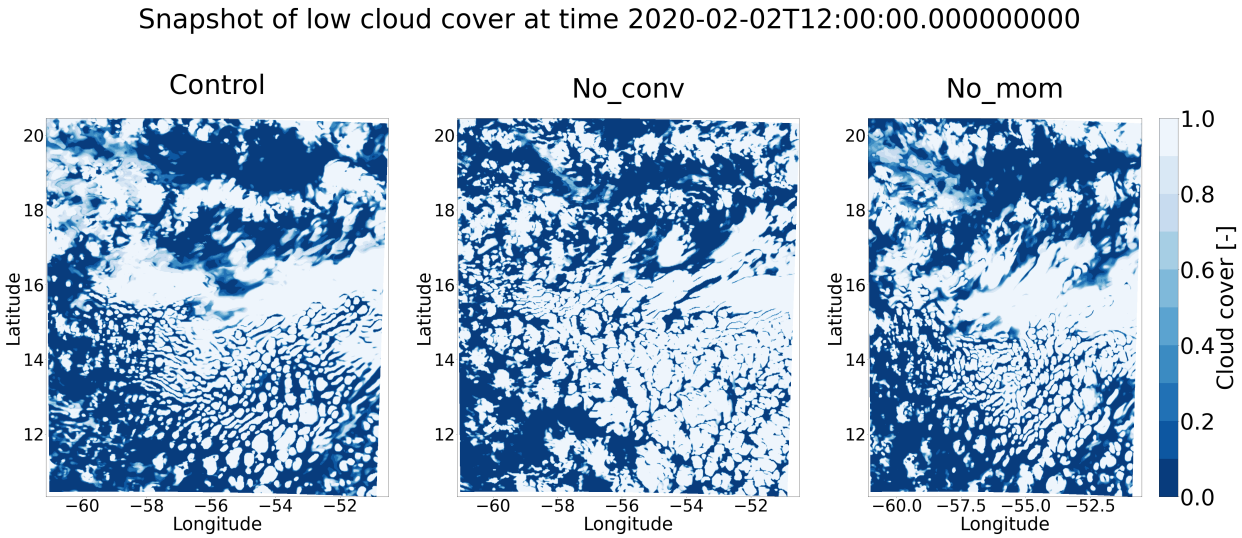

Figure 32: HARMONIE Snapshot of Low Cloud Cover for Control (Left Panel), No_conv (Middle Panel), No_mom (Right Panel) at Time 2020-02-02T12:00:00.

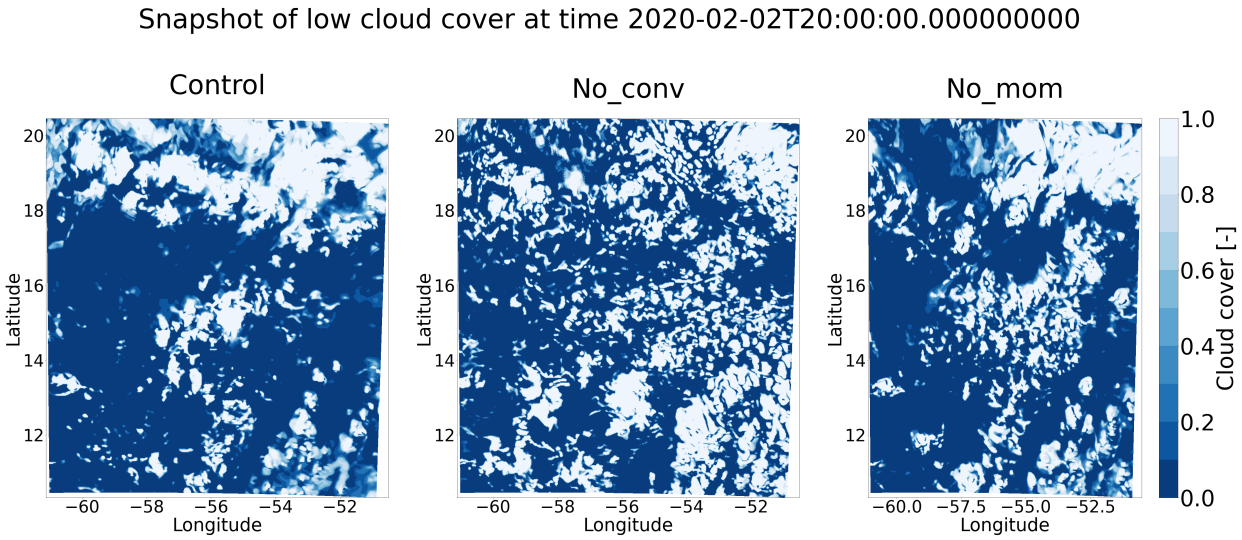

Figure 33: HARMONIE Snapshot of Low Cloud Cover for Control (Left Panel), No_conv (Middle Panel), No_mom (Right Panel) at Time 2020-02-02T20:00:00.

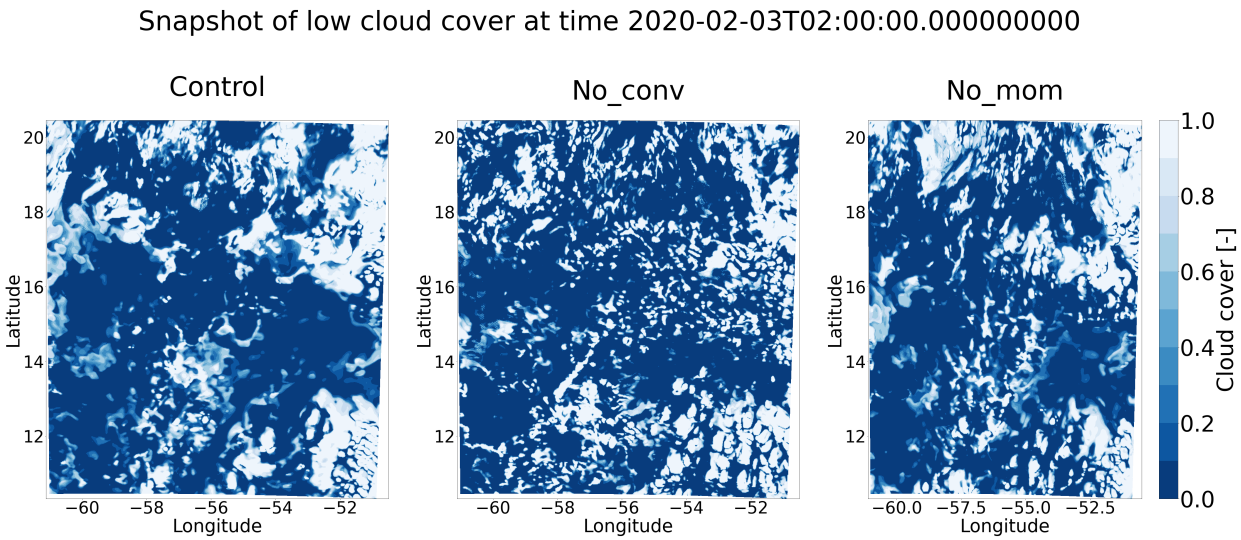

Figure 34: HARMONIE Snapshot of Low Cloud Cover for Control (Left Panel), No_conv (Middle Panel), No_mom (Right Panel) at Time 2020-02-03T02:00:00.

From the Figures (top row) it can be seen that none of the HARMONIE experiments are able to produce the fine sugar clouds that are present on 02/02/2020. This can be mainly attributed to the spatial resolution of the model, which is not able to reproduce such small scale fine clouds.

The analysis of the cloud pattern evolution in the 'control' experiment (left column) reveals interesting observations. While the experiment cannot fully reproduce the sugar pattern, there is a noticeable transition in the cloud organization from 02/02/2020 12:00 UTC to 02/02/2020 20:00 UTC. During this period, the clouds show a tendency to form slight clusters, resembling a pattern similar to the flower pattern. This transition in cloud organization indicates that the model's dynamics are capable of capturing some aspects of cloud clustering and organization, even if they do not precisely match the pattern.

In the 'no_conv' experiment (middle column), there is no clear and explicit transition from the sugar pattern to the flower pattern. However, similar to the 'control' experiment, some degree of clustering can still be seen in the Figure at 02/02/2020 20:00 UTC. Notably, the 'no_conv' experiment generates more cloud entities compared to the 'control' experiment, and these clouds tend to be more clustered. Moreover, the cloud organization in the 'no_conv' experiment appears to exhibit minimal day-to-day variation, suggesting a relatively stable cloud pattern in the absence of shallow convective parametrization.

Lastly, the 'no_mom' experiment (right column), similar to the 'control' and 'no_conv' experiments, exhibits no distinct transition from the sugar pattern to the flower pattern during the times presented.

6 Conclusions & Recommendations

To better understand the role of shallow convection in the weather system, three experiments have been conducted with the weather model HARMONIE; HARMONIE noHGTQS, HARMONIE noHGTQS noSHAL and HARMONIE noHGTQS noUVmix. This study analyses and compares these experiments with each other and to observational data. The major differences are summarized and explained below:

Various cloud organization metrics have been calculated using the outputs of low cloud cover from all of the experiments, focusing on the region of the North Atlantic trade-wind. These metrics provide objective and quantitative insights into the spatial patterns, arrangement, and structure of the low clouds in this region. By analyzing these metrics, we can gain a deeper understanding of how the cloud organization varies across the different experiments and assess the impact of different factors on the overall organization of low clouds in the North Atlantic trade-wind region.

The diurnal cycle of all computed metrics reveal a significant disparity between experiments and observations. For cloud cover the experiments show a mean of approximately 34% altogether, while the observational mean computed from the GOES-16 cloud and moisture data is 18%. Despite this deviation, the observations align with previous literature, which brings into question the ability of GOES-16 to accurately detect low cloud cover. This also indicates the possible need for a satellite simulator within HARMONIE. By incorporating a satellite simulator within the model it is possible to observe what satellites will potentially observe under the same atmospheric conditions of the model. This allows for a more useful comparison between the model and observations.

Due to the limitations of GOES-16 in detecting low clouds, additional data from the ceilometer has been utilized. Comparing the ceilometer data with the simulated data reveals a closer alignment. The 'no_conv' experiment excels in capturing the pattern and magnitude of the diurnal cycle from the ceilometer data. In contrast, the other experiments overestimate the amplitude of the diurnal cycle. It can also be observed that the values of cloud cover for the 'control' and the 'no_mom' experiments have larger differences during the night than during the day.

When it comes to open sky and number of objects both the 'control' and the 'no_mom' experiments capture the diurnal pattern, albeit with notable differences in magnitude. The key distinction among the experiments lies in the size and the quantity of cloud entities generated. The 'no_conv' experiment produces clouds that are smaller in size and approximately double the number of objects compared to the other experiments. This experiment outperforms the others in number of objects, by providing the best agreement with the observed values. Nevertheless, it fails to reproduce the full range of variability observed. This raises the question of how shallow convective parametrization exerts such a significant cloud production.

By disabling the parametrization of shallow convection, the continuous mixing of the atmosphere is halted. This interruption in mixing allows for the build-up of instability within a gridbox. Once this instability reaches a critical threshold, the resolved convection dissipates it, making the entire gridbox cloudy. This process occurs rapidly and at multiple locations throughout the domain, resulting in a significantly higher cloud count compared to the other experiments. Following the build up of instability, updrafts become stronger and clouds deeper. This phenomenon leads to an overall increase in cloud water content and therefore also more precipitation.

The primary focus of this research centered around the organization and patterns exhibited by clouds. Currently Iorg stands out as one of the most commonly employed metrics for assessing

the degree of cloud organization. HARMONIE is not able to accurately simulate the observed diurnal cycle of Iorg, while LES simulations replicate this. Based on the differences in resolutions one can conclude that the coarse resolution of HARMONIE is the primary reason it cannot replicate this Iorg diurnal pattern. Even though Iorg is widely used to determine the level of organization within cloud fields it is questioned whether it is the best way to quantify and describe organization. Cloud fields that visually have very different cloud patterns can have the same value of Iorg, which makes it difficult to interpret.

Overall, the impact of momentum mixing by wind on cloud production and the vertical profiles of various parameters is minimal compared to the influence of disabling shallow convection. The effect of momentum mixing is more apparent during nighttime, particularly on cloud cover. As anticipated, it does influence the wind patterns, resulting in weaker winds compared to the other experiments. These weaker winds can subsequently affect other aspects of the experiment such as precipitation. By disabling momentum mixing there is lower precipitation amounts compared to the 'control' experiment. This suggests that the mixing of momentum by wind affects the vertical transport of moisture and contributes to reduced precipitation production. This highlights the interconnected nature of different atmospheric variables and their influence on overall dynamics.

Based on the results it can be concluded that the 'no_conv' experiment demonstrates the most promising performance in some aspects, specifically in cloud cover and number of cloud entities produced. It is surprising that the 'control' experiment, currently in operation by the KNMI for regional weather forecasting, is not the best. One would expect since it is in operation. To begin with, the model was created with a primary focus on providing high-resolution weather forecasts and simulations for Europe and its surrounding areas. While it might excel in predicting weather and climate within that region, its effectiveness could vary in the North Atlantic and subtropical areas. This is due to dissimilarities in convection patterns and atmospheric dynamics between these regions. Furthermore, parameterizations are based on assumptions and simplifications, which can introduce biases into the model's outputs. By disabling the shallow convection parameterization, the model relies more on resolving physical processes directly, thus reducing the potential for biases introduced by parameterized equations. Convection-permitting models are designed to explicitly capture convective processes, including shallow convection. Therefore, when parameterizations are turned off, the model's representation of these processes becomes more consistent with actual observations, leading to results that better reflect real-world conditions.

While the 'no_conv' experiment may yield better results there is still room for improvement to achieve a comprehensive and precise simulation of the observed diurnal cycles. For this it is worth considering the potential benefits of implementing a combination of active and non-active shallow convective parametrization. Studies conducted by Khain et al. (2020) have demonstrated positive outcomes when employing such a hybrid approach. Therefore, investigating the feasibility and effectiveness of such a configuration within HARMONIE could provide valuable insights into improving the representation of cloud dynamics for the North Atlantic trade-wind region.

The model's resolution poses limitations in capturing small-scale and intricate cloud structures, such as those resembling sugar-like formations. While the model struggles to reproduce these detailed cloud features, it does exhibit a modest level of day-to-day variability in cloud patterns. Overall, while the HARMONIE experiments may fall short in accurately simulating small-scale cloud structures, they do exhibit a degree of variability in cloud patterns, presenting a progression from larger cloud structures to smaller clustered entities.

In order to gain a deeper understanding of the inter-experimental differences observed, it is advisable to conduct a more comprehensive investigation into the model configurations. It is essential to delve deeper into the dynamics of momentum mixing to gain a more comprehensive understanding of its effects, particularly exploring the reasons behind its heightened influence during nighttime. This could involve analyzing the role of surface cooling, boundary layer dynamics, and the interaction between momentum and temperature gradients. It can also be valuable to investigate how the absence of momentum mixing affects turbulent exchange processes during the night, because turbulence is a key driver of vertical mixing of heat, moisture, and momentum within the boundary layer which can affect several properties such as cloud cover.

Finally, in order to objectively assess the frequency of occurrence of the various patterns, it is proposed to utilize existing and trained neural networks. These neural networks, as referenced in Rasp et al. and Schulz, can be employed to analyze the cloud fields produced by the experiments and determine the number of recognized patterns. The neural networks employ sophisticated pattern recognition algorithms to identify and classify different types of cloud structures. Passing the simulated cloud fields of the HARMONIE experiments through these networks will provide insights into the extent to which the model can accurately replicate known cloud patterns and the frequency at which they occur.

Appendix A Metrics Complete Time-Series

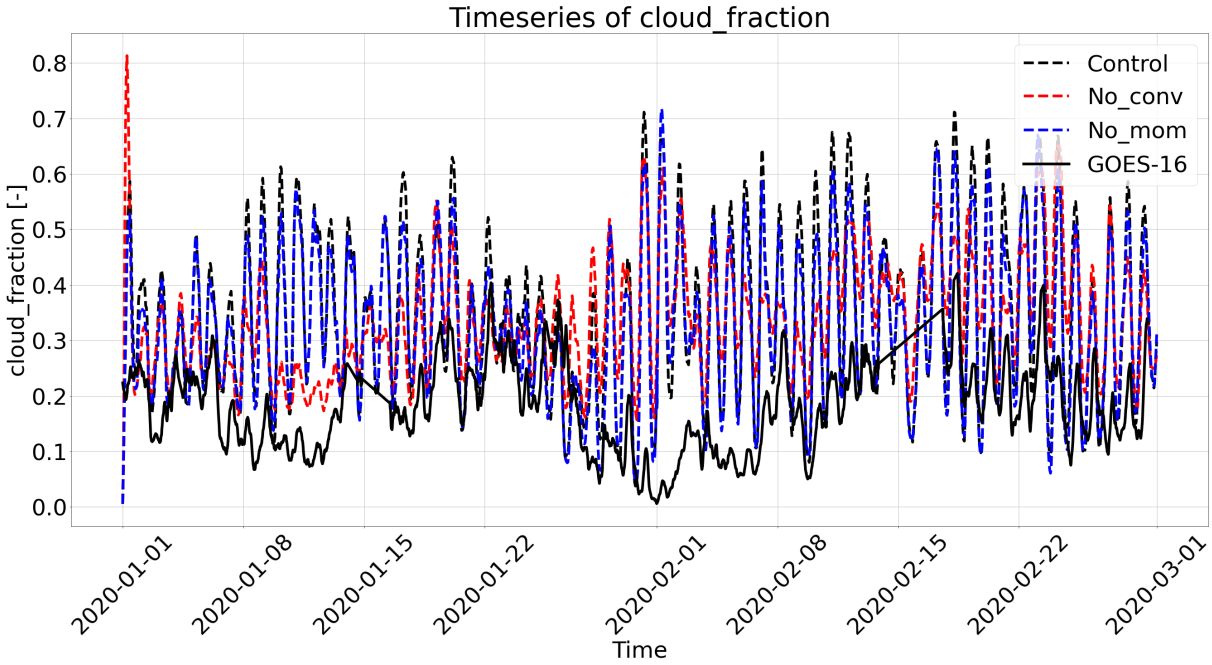

Figure 35: Complete Time-Series of the Low Cloud Cover Metric Using the Cloud Organization Algorithm.

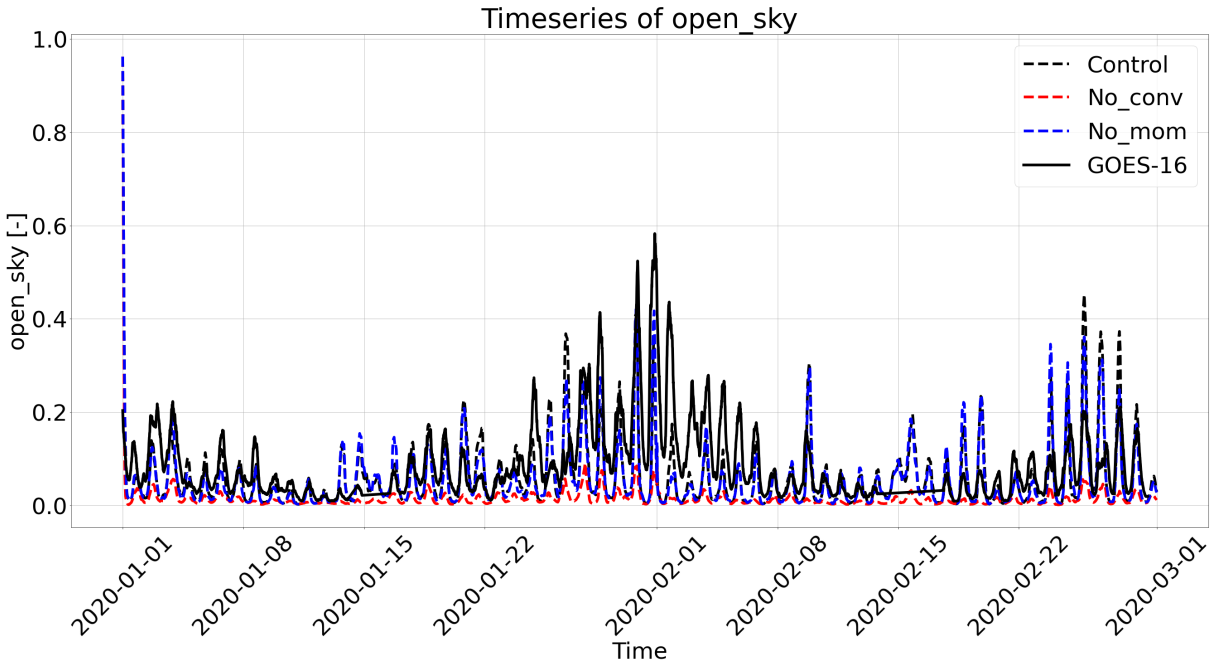

Figure 36: Complete Time-Series of the Open Sky Metric Using the Cloud Organization Algorithm.

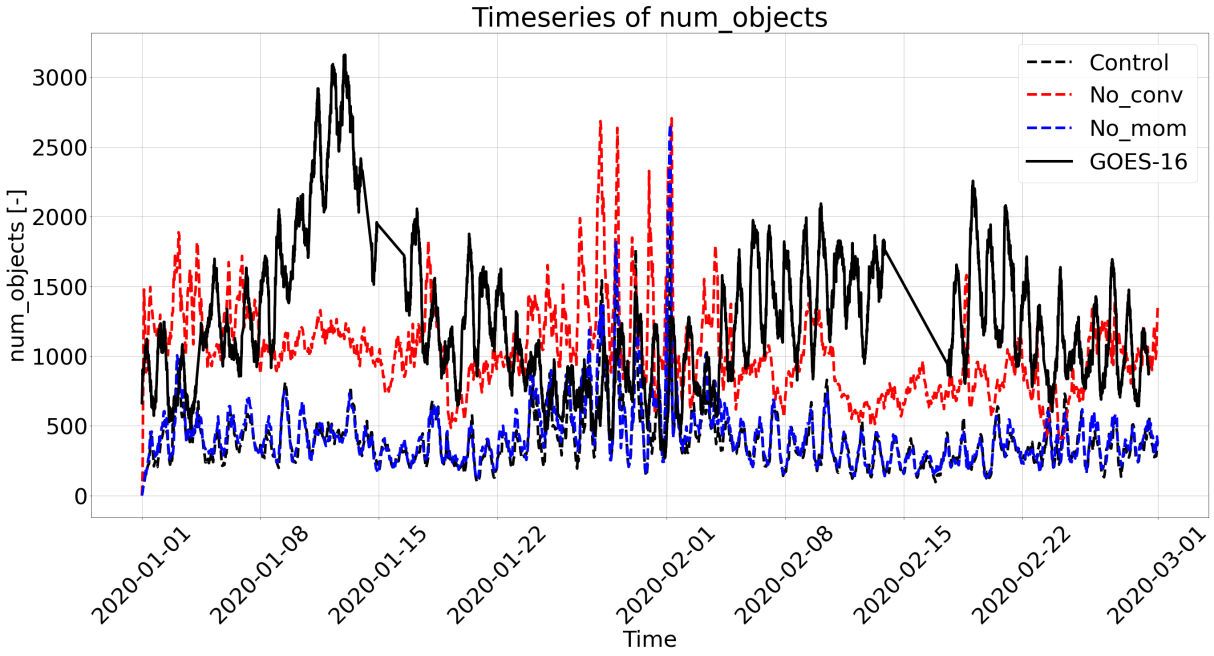

Figure 37: Complete Time-Series of the Number of Objects Metric Using the Cloud Organization Algorithm.

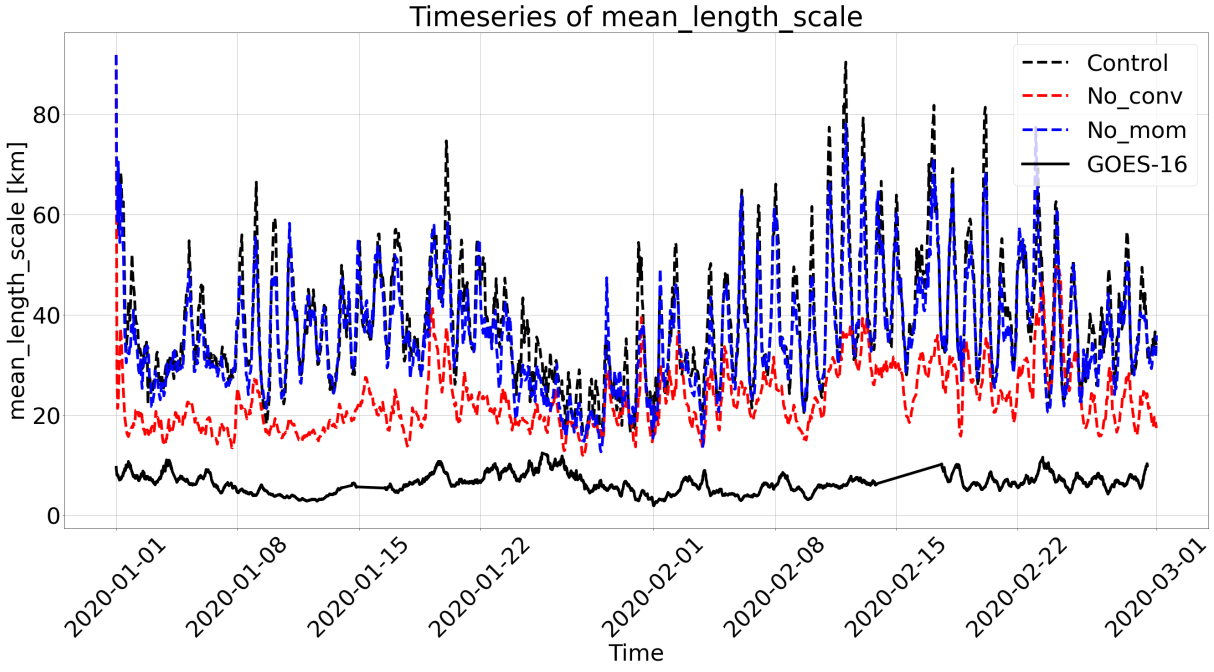

Figure 38: Complete Time-Series of the Mean Length Scale Metric Using the Cloud Organization Algorithm.

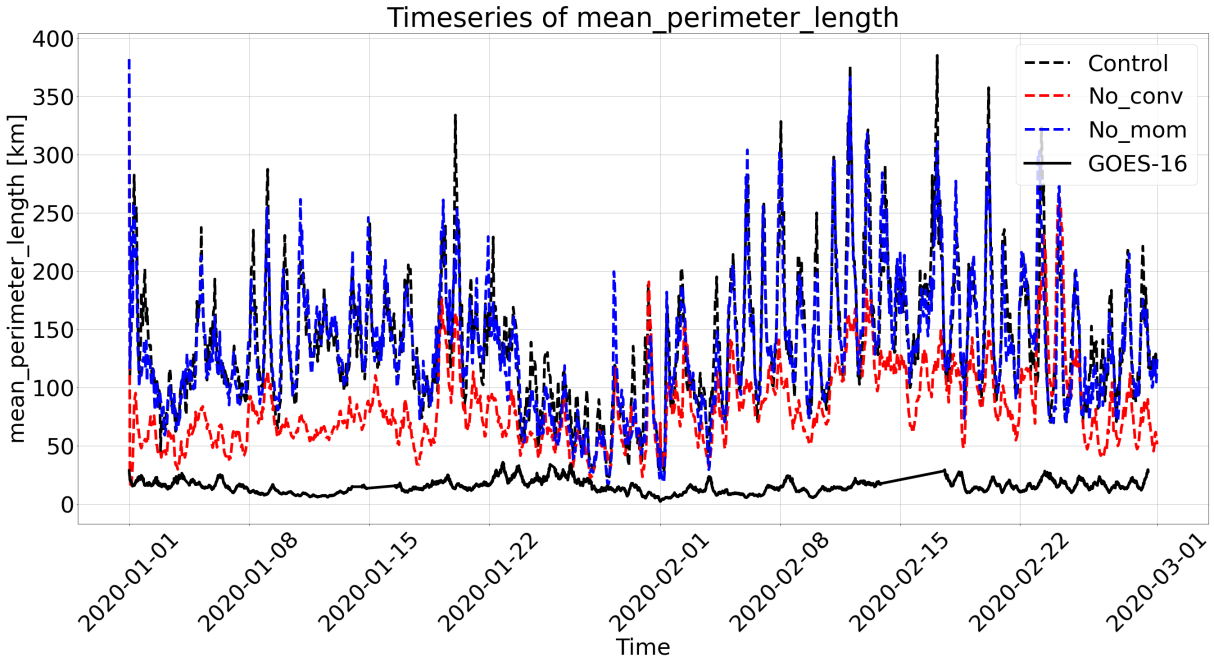

Figure 39: Complete Time-Series of the Mean Perimeter Length Metric Using the Cloud Organization Algorithm.

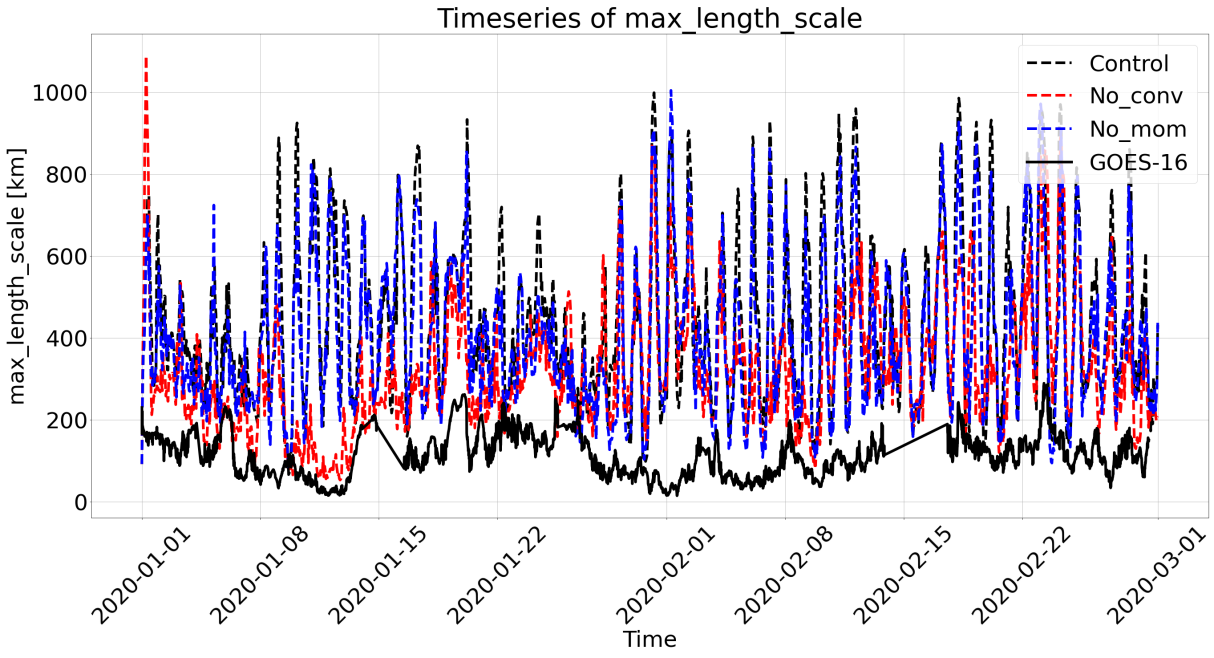

Figure 40: Complete Time-Series of the Maximum Length Scale Metric Using the Cloud Organization Algorithm.

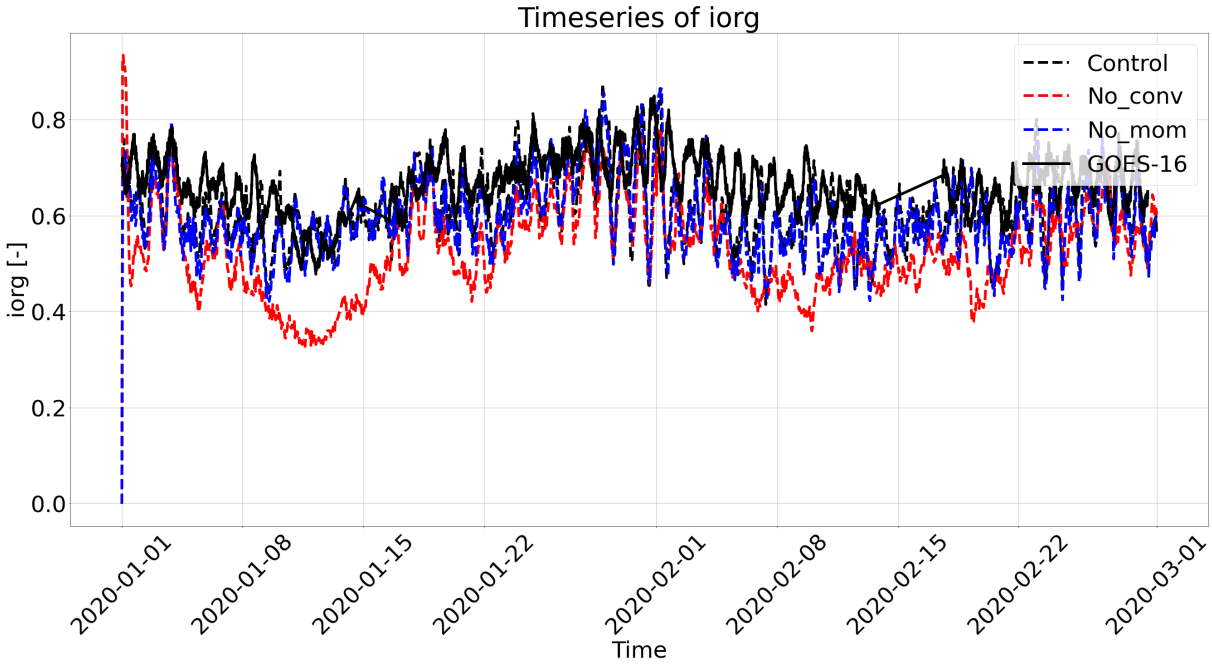

Figure 41: Complete Time-Series of the Cloud Organization Index Metric Using the Cloud Organization Algorithm.

References

[1] Moustafa T Chahine. *The hydrological cycle and its influence on climate*. 1992. DOI: https://doi.org/10.1038/359373a0.

[2] J T Kiehl and Kevin E Trenberth. *Earth's Annual Global Mean Energy Budget*. 1997. DOI: https://doi.org/10.1175/1520-0477(1997)078<0197:EAGMEB>2.0.CO;2.

[3] Sandrine Bony et al. *Clouds, circulation and climate sensitivity*. Apr. 2015, pp. 261–268. DOI: https://doi.org/10.1038/ngeo2398.

[4] B. W. Atkinson and J. Wu Zhang. *Mesoscale shallow convection in the atmosphere*. 4. 1996, pp. 403–431. DOI: https://doi.org/10.1029/96RG02623. eprint: https://agupubs.onlinelibrary.wiley.com/doi/pdf/10.1029/96RG02623. URL: https://agupubs.onlinelibrary.wiley.com/doi/abs/10.1029/96RG02623.

[5] Peter M. Caldwell et al. "Quantifying the Sources of Intermodel Spread in Equilibrium Climate Sensitivity". In: *Journal of Climate* 29.2 (2016), pp. 513–524. DOI: https://doi.org/10.1175/JCLI-D-15-0352.1. URL: https://journals.ametsoc.org/view/journals/clim/29/2/jcli-d-15-0352.1.xml.

[6] IPCC. "2022: Summary for Policymakers [H.-O. Pörtner, D.C. Roberts, E.S. Poloczanska, K. Mintenbeck, M. Tignor, A. Alegría, M. Craig, S. Langsdorf, S. Löschke, V. Möller, A. Okem (eds.)]. In: *Climate Change 2022: Impacts, Adaptation and Vulnerability*. Contribution of Working Group II to the Sixth Assessment Report of the Intergovernmental Panel on Climate Change [H.-O. Pörtner, D.C. Roberts, M. Tignor, E.S. Poloczanska, K. Mintenbeck, A. Alegría, M. Craig, S. Langsdorf, S. Löschke, V. Möller, A. Okem, B. Rama (eds.)]" In: (2022). DOI: https://doi.org/10.1017/9781009325844.001.

[7] Abdul Azim Amirudin et al. "The Importance of Cumulus Parameterization and Resolution in Simulating Rainfall over Peninsular Malaysia". In: *Atmosphere* 13.10 (Sept. 2022), p. 1557. DOI: https://doi.org/10.3390/atmos13101557.

[8] Hannah Christensen and Laure Zanna. "Parametrization in Weather and Climate Models". In: (Dec. 2022). DOI: https://doi.org/10.1093/acrefore/9780190228620.013.826. URL: https://oxfordre.com/climatescience/view/10.1093/acrefore/9780190228620.001.0001/acrefore-9780190228620-e-826.

[9] Louise Nuijens and A.P. Siebesma. "Boundary Layer Clouds and Convection over Subtropical Oceans in our Current and in a Warmer Climate". In: *Current Climate Change Reports* 5 (June 2019), pp. 1–15. DOI: https://doi.org/10.1007/s40641-019-00126-x.

[10] *International Cloud Atlas*. World Meteorological Organization, 1975.

[11] JOSHUA Z. HOLLAND and EUGENE M. RASMUSSON. "Measurements of the Atmospheric Mass, Energy, and Momentum Budgets Over a 500-Kilometer Square of Tropical Ocean". In: *Monthly Weather Review* 101.1 (1973), pp. 44–55. DOI: https://doi.org/10.1175/1520-0493(1973)101<0044:MOTAME>2.3.CO;2. URL: https://journals.ametsoc.org/view/journals/mwre/101/1/1520-0493_1973_101_0044_motame_2_3_co_2.xml.

[12] Bruce A. Albrecht et al. "The Atlantic Stratocumulus Transition Experiment—ASTEX". In: *Bulletin of the American Meteorological Society* 76.6 (1995), pp. 889–904. DOI: https://doi.org/10.1175/1520-0477(1995)076<0889:TASTE>2.0.CO;2. URL: https://journals.ametsoc.org/view/journals/bams/76/6/1520-0477_1995_076_0889_taste_2_0_co_2.xml.

[13] Robert M. Rauber et al. "Rain in Shallow Cumulus Over the Ocean: The RICO Campaign". In: *Bulletin of the American Meteorological Society* 88.12 (2007), pp. 1912–1928. DOI: https://doi.org/10.1175/BAMS-88-12-1912. URL: https://journals.ametsoc.org/view/journals/bams/88/12/bams-88-12-1912.xml.

[14] B. Stevens et al. "EUREC^{4}A". In: *Earth System Science Data* 13.8 (2021), pp. 4067–4119. DOI: 10.5194/essd-13-4067-2021. URL: https://essd.copernicus.org/articles/13/4067/2021/.

[15] Sandrine Bony et al. "EUREC4A: A Field Campaign to Elucidate the Couplings Between Clouds, Convection and Circulation". In: Jan. 2017, pp. 357–396. ISBN: 978-3-319-77272-1. DOI: 10.1007/978-3-319-77273-8_16.

[16] Brian Medeiros and Louise Nuijens. "Clouds at Barbados are representative of clouds across the trade wind regions in observations and climate models". In: *Proceedings of the National Academy of Sciences* 113.22 (2016), E3062–E3070. DOI: 10.1073/pnas.1521494113. eprint: https://www.pnas.org/doi/pdf/10.1073/pnas.1521494113. URL: https://www.pnas.org/doi/abs/10.1073/pnas.1521494113.

[17] P. Bechtold et al. *The role of shallow convection in ECMWFs integrated forecasting system*. July 2014.

[18] Bjorn Stevens et al. "Sugar, gravel, fish and flowers: Mesoscale cloud patterns in the trade winds". In: *Quarterly Journal of the Royal Meteorological Society* 146.726 (2020), pp. 141–152. DOI: https://doi.org/10.1002/qj.3662. eprint: https://rmets.onlinelibrary.wiley.com/doi/pdf/10.1002/qj.3662. URL: https://rmets.onlinelibrary.wiley.com/doi/abs/10.1002/qj.3662.

[19] Kevin C. Helfer, Louise Nuijens, and Vishal V. Dixit. "The role of shallow convection in the momentum budget of the trades from large-eddy-simulation hindcasts". In: *Quarterly Journal of the Royal Meteorological Society* 147.737 (2021), pp. 2490–2505. DOI: https://doi.org/10.1002/qj.4035. eprint: https://rmets.onlinelibrary.wiley.com/doi/pdf/10.1002/qj.4035. URL: https://rmets.onlinelibrary.wiley.com/doi/abs/10.1002/qj.4035.

[20] Bjorn Stevens et al. "The Barbados cloud observatory: Anchoring investigations of clouds and circulation on the edge of the itcz". In: *Bulletin of the American Meteorological Society* 97 (5 2016). ISSN: 00030007. DOI: 10.1175/BAMS-D-14-00247.1.

[21] Fieneke van der Voort. *Evaluation of the representation of subtropical marine clouds in the numerical weather prediction model HARMONIE*. 2021.

[22] Coco Antonissen. *Organization of Cumulus Convection over (sub)tropical oceans*. Apr. 2019.

[23] L. Nuijens et al. "The distribution and variability of low-level cloud in the North Atlantic trades". In: *Quarterly Journal of the Royal Meteorological Society* 140.684 (2014), pp. 2364–2374. DOI: https://doi.org/10.1002/qj.2307. eprint: https://rmets.onlinelibrary.wiley.com/doi/pdf/10.1002/qj.2307. URL: https://rmets.onlinelibrary.wiley.com/doi/abs/10.1002/qj.2307.

[24] Physical Sciences Laboratory. URL: https://psl.noaa.gov/atomic/ (visited on 05/24/2023).

[25] L. Denby. "Discovering the Importance of Mesoscale Cloud Organization Through Unsupervised Classification". In: *Geophysical Research Letters* 47 (1 Jan. 2020). ISSN: 19448007. DOI: https://doi.org/10.1029/2019GL085190.

[26] Stephan Rasp et al. "Combining crowd-sourcing and deep learning to understand mesoscale organization of shallow convection". In: *Bulletin of the American Meteorological Society* (June 2019). DOI: 10.1175/BAMS-D-19-0324.1.

[27] Martin Janssens et al. "Cloud Patterns in the Trades Have Four Interpretable Dimensions". In: *Geophysical Research Letters* 48 (Mar. 2021). DOI: https://doi.org/10.1029/2020GL091001.

[28] Jessica Vial, Raphaela Vogel, and Hauke Schulz. "On the daily cycle of mesoscale cloud organization in the winter trades". In: *Quarterly Journal of the Royal Meteorological Society* 147.738 (2021), pp. 2850–2873. DOI: https://doi.org/10.1002/qj.4103. eprint: https://rmets.onlinelibrary.wiley.com/doi/pdf/10.1002/qj.4103. URL: https://rmets.onlinelibrary.wiley.com/doi/abs/10.1002/qj.4103.

[29] Jessica Vial et al. "A New Look at the Daily Cycle of Trade Wind Cumuli". In: *Journal of Advances in Modeling Earth Systems* 11.10 (2019), pp. 3148–3166. DOI: https://doi.org/10.1029/2019MS001746. eprint: https://agupubs.onlinelibrary.wiley.com/doi/pdf/10.1029/2019MS001746. URL: https://agupubs.onlinelibrary.wiley.com/doi/abs/10.1029/2019MS001746.

[30] Jessica Vial et al. "Cloud transition across the daily cycle illuminates model responses of trade cumuli to warming". In: *Proceedings of the National Academy of Sciences* 120.8 (2023), e2209805120. DOI: 10.1073/pnas.2209805120. eprint: https://www.pnas.org/doi/pdf/10.1073/pnas.2209805120. URL: https://www.pnas.org/doi/abs/10.1073/pnas.2209805120.

[31] Jose A. Garcia-Moya et al. *Deterministic and probabilistic weather forecasting*. July 2016, pp. 9–15.

[32] B. Stevens et al. "EUREC^{4}A". In: *Earth System Science Data* 13.8 (2021), pp. 4067–4119. DOI: 10.5194/essd-13-4067-2021. URL: https://essd.copernicus.org/articles/13/4067/2021/.

[33] W. C. de Rooy et al. "Model development in practice: a comprehensive update to the boundary layer schemes in HARMONIE-AROME cycle 40". In: *Geoscientific Model Development* 15.4 (2022), pp. 1513–1543. DOI: 10.5194/gmd-15-1513-2022. URL: https://gmd.copernicus.org/articles/15/1513/2022/.

[34] G. Liberia. *A validation of subtropical marine low clouds in the HARMONIE regional weather model*. 2023. URL: http://resolver.tudelft.nl/uuid:d9a02568-7353-4440-b1a2-cad02d1fd82e.

[35] John Marshall and R. Alan Plumb. eng. In: *Atmosphere, Ocean and Climate Dynamics*. Academic Press, Jan. 1969, p. 48. URL: https://www.123library.org/ebook/isbn/9780080954493/.

[36] https://www.wpc.ncep.noaa.gov/international/training/deep/sld004.htm. Accessed: 2023-05-09.

[37] Lisa Bengtsson et al. "The HARMONIE–AROME Model Configuration in the ALADIN–HIRLAM NWP System". In: *Monthly Weather Review* 145.5 (2017), pp. 1919–1935. DOI: 10.1175/MWR-D-16-0417.1. URL: https://journals.ametsoc.org/view/journals/mwre/145/5/mwr-d-16-0417.1.xml.

[38] Arnold F. Moene and Jos C. van Dam. *Transport in the Atmosphere-Vegetation-Soil Continuum*. Cambridge University Press, 2014. DOI: 10.1017/CBO9781139043137.

[39] A. P. Siebesma. "Shallow Cumulus Convection". In: *Buoyant Convection in Geophysical Flows*. Ed. by E. J. Plate et al. Dordrecht: Springer Netherlands, 1998, pp. 441–486. ISBN: 978-94-011-5058-3. DOI: 10.1007/978-94-011-5058-3_19. URL: https://doi.org/10.1007/978-94-011-5058-3_19.

[40] Pavel Khain et al. "Effect of shallow convection parametrization on cloud resolving NWP forecasts over the Eastern Mediterranean". In: *Atmospheric Research* 247 (Aug. 2020), p. 105213. DOI: 10.1016/j.atmosres.2020.105213.

[41] NOAA Comprehensive Large Array Data Stewardship System. URL: https://www.avl.class.noaa.gov/saa/products/welcome;jsessionid=73E0AB2EF70FC1EFF250480525CA57AB (visited on 05/24/2023).

[42] R. C. Weger et al. "Clustering, randomness and regularity in cloud fields: 1. Theoretical considerations". In: *Journal of Geophysical Research: Atmospheres* 97.D18 (1992), pp. 20519–20536. DOI: https://doi.org/10.1029/92JD02038. eprint: https://agupubs.onlinelibrary.wiley.com/doi/pdf/10.1029/92JD02038. URL: https://agupubs.onlinelibrary.wiley.com/doi/abs/10.1029/92JD02038.

[43] Timothy C. Benner and Judith A. Curry. "Characteristics of small tropical cumulus clouds and their impact on the environment". In: *Journal of Geophysical Research: Atmospheres* 103.D22 (1998), pp. 28753–28767. DOI: https://doi.org/10.1029/98JD02579. eprint: https://agupubs.onlinelibrary.wiley.com/doi/pdf/10.1029/98JD02579. URL: https://agupubs.onlinelibrary.wiley.com/doi/abs/10.1029/98JD02579.

[44] Adrian M. Tompkins and Addisu G. Semie. "Organization of tropical convection in low vertical wind shears: Role of updraft entrainment". In: *Journal of Advances in Modeling Earth Systems* 9.2 (2017), pp. 1046–1068. DOI: https://doi.org/10.1002/2016MS000802. eprint: https://agupubs.onlinelibrary.wiley.com/doi/pdf/10.1002/2016MS000802. URL: https://agupubs.onlinelibrary.wiley.com/doi/abs/10.1002/2016MS000802.

[45] Sandrine Bony et al. "Sugar, Gravel, Fish, and Flowers: Dependence of Mesoscale Patterns of Trade-Wind Clouds on Environmental Conditions". In: *Geophysical Research Letters* 47.7 (2020). e2019GL085988 10.1029/2019GL085988, e2019GL085988. DOI: https://doi.org/10.1029/2019GL085988. eprint: https://agupubs.onlinelibrary.wiley.com/doi/pdf/10.1029/2019GL085988. URL: https://agupubs.onlinelibrary.wiley.com/doi/abs/10.1029/2019GL085988.

[46] Pornampai Narenpitak et al. "From Sugar to Flowers: A Transition of Shallow Cumulus Organization During ATOMIC". In: *Journal of Advances in Modeling Earth Systems* 13.10 (2021). e2021MS002619 2021MS002619, e2021MS002619. DOI: https://doi.org/10.1029/2021MS002619. eprint: https://agupubs.onlinelibrary.wiley.com/doi/pdf/10.1029/2021MS002619. URL: https://agupubs.onlinelibrary.wiley.com/doi/abs/10.1029/2021MS002619.

[47] Pedro A. Jiménez. "Assessment of the GOES-16 Clear Sky Mask Product over the Contiguous USA Using CALIPSO Retrievals". In: *Remote Sensing* 12.10 (2020). ISSN: 2072-4292. DOI: 10.3390/rs12101630. URL: https://www.mdpi.com/2072-4292/12/10/1630.

[48] A. C. M. Savazzi et al. "The representation of the trade winds in ECMWF forecasts and reanalyses during EUREC^{4}A". In: *Atmospheric Chemistry and Physics* 22.19 (2022), pp. 13049–13066. DOI: 10.5194/acp-22-13049-2022. URL: https://acp.copernicus.org/articles/22/13049/2022/.

[49] James H. Ruppert and Richard H. Johnson. "On the cumulus diurnal cycle over the tropical warm pool". In: *Journal of Advances in Modeling Earth Systems* 8.2 (2016), pp. 669–690. DOI: https://doi.org/10.1002/2015MS000610. eprint: https://agupubs.onlinelibrary.wiley.com/doi/pdf/10.1002/2015MS000610. URL: https://agupubs.onlinelibrary.wiley.com/doi/abs/10.1002/2015MS000610.

[50] Raphaela Vogel, Sandrine Bony, and Bjorn Stevens. "Estimating the Shallow Convective Mass Flux from the Subcloud-Layer Mass Budget". In: *Journal of the Atmospheric Sciences* 77.5 (2020), pp. 1559–1574. DOI: https://doi.org/10.1175/JAS-D-19-0135.1. URL: https://journals.ametsoc.org/view/journals/atsc/77/5/jas-d-19-0135.1.xml.

[51] Louise Nuijens, Bjorn Stevens, and A. Pier Siebesma. "The Environment of Precipitating Shallow Cumulus Convection". In: *Journal of the Atmospheric Sciences* 66.7 (2009), pp. 1962–1979. DOI: https://doi.org/10.1175/2008JAS2841.1. URL: https://journals.ametsoc.org/view/journals/atsc/66/7/2008jas2841.1.xml.

[52] H. Schulz. "C^{3}ONTEXT: a Common Consensus on Convective OrgaNizaTion during the EUREC^{4}A eXperimenT". In: *Earth System Science Data* 14.3 (2022), pp. 1233–1256. DOI: 10.5194/essd-14-1233-2022. URL: https://essd.copernicus.org/articles/14/1233/2022/.